

NASA-CR-190,347

SC73001.FR

NASA-CR-190347
19920016772

SC73001.FR

Copy No. 3

MAGNETIC FIELD EFFECTS ON MICROWAVE ABSORBING MATERIALS

FINAL REPORT FOR PERIOD:
November 1, 1988 through January 31, 1990

SUBCONTRACT NO. 535559
NASA GRANT NSG-1613
GENERAL ORDER 73001

Prepared for:

Ohio State Research Foundation
ElectroScience Laboratory
1320 Kinnear Road
Columbus, OH 43212-1194

by:

Ira Goldberg, Charles S. Hollingsworth and Ted M.
McKinney
Rockwell International Science Center
Thousand Oaks, CA 91360

APRIL 1991



**Rockwell International
Science Center**

LIBRARY COPY

6 1994

LANGLEY RESEARCH CENTER
LIBRARY NASA
HAMPTON, VIRGINIA

(NASA-CR-190347) MAGNETIC FIELD EFFECTS ON
MICROWAVE ABSORBING MATERIALS Final Report,
1 Nov. 1988 - 31 Jan. 1990 (Rockwell
International Science Center) 73 p

N92-26015

Unclas
G3/32 0091388

DISPLAY 92N26015/2

92N26015*# ISSUE 16 PAGE 2733 CATEGORY 32

RPT#: NASA-CR-190347 NAS 1.26:190347 SC#3001.FR CNT#: NSG-1613

91/04/00 73 PAGES UNCLASSIFIED DOCUMENT

UTTL: Magnetic field effects on microwave absorbing materials TLSP: Final
Report, 1 Nov. 1988 - 31 Jan. 1990

AUTH: A/GOLDBERG, IRA; B/HOLLINGSWORTH, CHARLES S.; C/MCKINNEY, TED M.

CORP: Rockwell International Science Center, Thousand Oaks, CA.; Ohio State
Univ., Columbus.

SAP: Avail: CASI HC A04/MF A01

CIO: UNITED STATES Prepared for Ohio State Univ., Columbus Original contains
color illustrations

MAJS: /*ABSORBERS (MATERIALS)/*FERRITES/*MAGNETIC EFFECTS/*MAGNETIC FIELDS/*
MAGNETIC PROPERTIES/*MICROWAVES/*NONUNIFORM MAGNETIC FIELDS

MINS: / COATINGS/ DIRECT CURRENT/ ELECTRIC FIELDS/ ELECTRICAL PROPERTIES/
MAGNETIC PERMEABILITY/ TRANSMISSION LINES

ABA: H.A.

ABS: The objective of this program was to gather information to formulate a
microwave absorber that can work in the presence of strong constant direct
current (DC) magnetic fields. The program was conducted in four steps. The
first step was to investigate the electrical and magnetic properties of
magnetic and ferrite microwave absorbers in the presence of strong
magnetic fields. This included both experimental measurements and a

ENTER: MORE

DISPLAY 92N26015/2

literature survey of properties that may be applicable to finding an appropriate absorbing material. The second step was to identify those material properties that will produce desirable absorptive properties in the presence of intense magnetic fields and determine the range of magnetic field in which the absorbers remain effective. The third step was to establish ferrite absorber designs that will produce low reflection and adequate absorption in the presence of intense inhomogeneous static magnetic fields. The fourth and final step was to prepare and test samples of such magnetic microwave absorbers if such designs seem practical.

ENTER:



TABLE OF CONTENTS

	<u>Page</u>
1.0 OBJECTIVE	1
2.0 INTRODUCTION	2
2.1 Magnetic Unites and Terminoloy	2
2.2 Magnetic Loop	3
2.3 Magnetic Permeability	7
3.0 RESULTS AND DISCUSSION	14
3.1 Concept for Preliminary Test	14
3.2 Experimental Methods	14
3.2.1 Transmission Line Measurements	14
3.2.2 Cavity Perturbation Measurements	16
3.2.3 Materials and Concentrations	17
3.3 Measurement Results	19
3.3.1 Transmission Line Measurements	19
3.3.2 Cavity Perturbation Measurements	31
4.0 CONCLUSIONS AND DISCUSSION OF RESULTS	54
4.1 General Performance	54
4.2 Coating Geometry and Orientation (a Cautionary Note)	55
4.3 Conclusions	57
5.0 RECOMMENDATIONS	59
5.1 Material and CIP Concentration	59
5.2 Measurements	59
6.0 REFERENCES	61
APPENDIX 1 - BIBLIOGRAPHY ON MICROWAVE MAGNETICS	62

ORIGINAL CONTAINS
COLOR PHOTOGRAPHS



LIST OF FIGURES

<u>Figure</u>		<u>Page</u>
1	M-H loops: (a) Typical moderate coercivity material; (b) Iron carbonyl powder exhibiting low coercivity (sample size approximately $1.2 \times 0.6 \times 0.055$ cm); and (c) Minor loop of b around small applied magnetic fields.	5
2	Schematic representation of the domain structure of (a) nonmagnetized magnetic material; (b) partially magnetized material; and (c) fully magnetized material.	7
3	Schematic drawing of the mechanism of eddy current losses due to a conductive magnetic particle in an oscillating magnetic field: (a) oscillating field induces magnetization in the particle; (b) magnetization creates internal flux density; and (c) currents are induced by the time dependent magnetic flux.	10
4	(a) Diagram of 7 mm coaxial transmission line cell and direction of the applied magnetic field; (b) Torroidal sample and dimensions; and (c) diagram of the applied magnetic field and the poles generated at the sample surface.	16
5	Plots of the real and imaginary parts of permeability determined on the empty transmission line cell as a function of frequency at: (a) 0 Oe; and (b) 12.5 kOe.	20
6	Plots of the real and imaginary parts of permeability and permittivity, respectively μ' , μ'' , ϵ' and ϵ'' vs frequency (GHz) for a mixture of 40% by volume HFQ grade carbonyl iron powder in epoxy at different applied magnetic fields: (a) real part of permeability, (b) imaginary part of permeability; (c) real part of permittivity; and (d) imaginary part of permittivity.	21
7	Plots of the real and imaginary parts of permeability, respectively μ' and μ'' , vs frequency (GHz) for a mixture of 30% by volume HFQ grade carbonyl iron powder in epoxy at different applied magnetic fields: (a) real part of permeability and (b) imaginary part of permeability.	22
8	Plots of the real and imaginary parts of permeability, respectively μ' and μ'' , vs frequency (GHz) for a mixture of 20% by volume HFQ grade carbonyl iron powder in epoxy at different applied magnetic fields: (a) real part of permeability and (b) imaginary part of permeability.	23



LIST OF FIGURES

<u>Figure</u>		<u>Page</u>
9	Plots of the real and imaginary parts of permeability, respectively μ' and μ'' , vs frequency (GHz) for a mixture of 40% by volume KX grade carbonyl iron powder in epoxy at different applied magnetic fields: (a) real part of permeability and (b) imaginary part of permeability.	24
10	Plots of the real and imaginary parts of permeability, respectively μ' and μ'' , vs frequency (GHz) for a mixture of 40% by volume SF grade carbonyl iron powder in epoxy at different applied magnetic fields: (a) real part of permeability and (b) imaginary part of permeability.	25
11	Plots of the real and imaginary parts of permeability, respectively μ' and μ'' , vs frequency (GHz) for a mixture of 20% by volume SF grade carbonyl iron powder in epoxy at different applied magnetic fields: (a) real part of permeability and (b) imaginary part of permeability.	26
12	Plots of the real and imaginary parts of permeability, respectively μ' and μ'' , vs frequency (GHz) for a mixture of 40% by volume TH grade carbonyl iron powder in epoxy at different applied magnetic fields: (a) real part of permeability and (b) imaginary part of permeability.	27
13	Plots of the real and imaginary parts of permeability, respectively μ' and μ'' , vs frequency (GHz) for a mixture of 30% by volume E grade carbonyl iron powder in epoxy at different applied magnetic fields: (a) real part of permeability and (b) imaginary part of permeability.	28
14	Plots of the real and imaginary parts of permeability, respectively μ' and μ'' , vs frequency (GHz) for a mixture of 20% by volume E grade carbonyl iron powder in epoxy at different applied magnetic fields: (a) real part of permeability and (b) imaginary part of permeability.	30
15	Results of cavity perturbation measurements at 9.5 GHz on a 0.5% by volume sample of carbonyl iron powder 60730-01 in epoxy: (a) frequency shift vs applied magnetic field; and (b) reciprocal of the sample Q-factor vs applied field.	32



LIST OF FIGURES

<u>Figure</u>		<u>Page</u>
16	Results of cavity perturbation measurements at 9.5 GHz on a 1.0% by volume sample of carbonyl iron powder 60730-01 in epoxy: (a) frequency shift vs applied magnetic field; and (b) reciprocal of the sample Q-factor vs applied field.	33
17	Results of cavity perturbation measurements at 9.5 GHz on a 2.0% by volume sample of carbonyl iron powder 60730-01 in epoxy: (a) frequency shift vs applied magnetic field; and (b) reciprocal of the sample Q-factor vs applied field.	34
18	Results of cavity perturbation measurements at 9.5 GHz on a 5.0% by volume sample of carbonyl iron powder 60730-01 in epoxy: (a) frequency shift vs applied magnetic field; and (b) reciprocal of the sample Q-factor vs applied field.	35
19	Results of cavity perturbation measurements at 9.5 GHz on a 0.5% by volume sample of carbonyl iron powder 60730-05 in epoxy: (a) frequency shift vs applied magnetic field; and (b) reciprocal of the sample Q-factor vs applied field.	37
20	Results of cavity perturbation measurements at 9.5 GHz on a 5.0% by volume sample of carbonyl iron powder 60730-05 in epoxy: (a) frequency shift vs applied magnetic field; and (b) reciprocal of the sample Q-factor vs applied field.	38
21	Results of cavity perturbation measurements at 9.5 GHz on a 0.5% by volume sample of carbonyl iron powder 60730-08 in epoxy: (a) frequency shift vs applied magnetic field; and (b) reciprocal of the sample Q-factor vs applied field.	39
22	Results of cavity perturbation measurements at 9.5 GHz on a 5.0% by volume sample of carbonyl iron powder 60730-08 in epoxy: (a) frequency shift vs applied magnetic field; and (b) reciprocal of the sample Q-factor vs applied field.	40
23	Results of cavity perturbation measurements at 9.5 GHz on a 0.5% by volume sample of carbonyl iron powder 60730-13 in epoxy: (a) frequency shift vs applied magnetic field; and (b) reciprocal of the sample Q-factor vs applied field.	41



LIST OF FIGURES

<u>Figure</u>		<u>Page</u>
24	Results of cavity perturbation measurements at 9.5 GHz on a 1.0% by volume sample of carbonyl iron powder 60730-13 in epoxy: (a) frequency shift vs applied magnetic field; and (b) reciprocal of the sample Q-factor vs applied field.	42
25	Results of cavity perturbation measurements at 9.5 GHz on a 2.0% by volume sample of carbonyl iron powder 60730-13 in epoxy: (a) frequency shift vs applied magnetic field; and (b) reciprocal of the sample Q-factor vs applied field.	43
26	Results of cavity perturbation measurements at 9.5 GHz on a 5.0% by volume sample of carbonyl iron powder 60730-13 in epoxy: (a) frequency shift vs applied magnetic field; and (b) reciprocal of the sample Q-factor vs applied field.	44
27	Results of cavity perturbation measurements at 9.5 GHz on a 0.5% by volume sample of GS6 carbonyl iron powder in epoxy: (a) frequency shift vs applied magnetic field; and (b) reciprocal of the sample Q-factor vs applied field.	45
28	Results of cavity perturbation measurements at 9.5 GHz on a 1.0% by volume sample of GS6 carbonyl iron powder in epoxy: (a) frequency shift vs applied magnetic field; and (b) reciprocal of the sample Q-factor vs applied field.	46
29	Results of cavity perturbation measurements at 9.5 GHz on a 2.0% by volume sample of GS6 carbonyl iron powder in epoxy: (a) frequency shift vs applied magnetic field; and (b) reciprocal of the sample Q-factor vs applied field.	47
30	Results of cavity perturbation measurements at 9.5 GHz on a 5.0% by volume sample of GS6 carbonyl iron powder in epoxy: (a) frequency shift vs applied magnetic field; and (b) reciprocal of the sample Q-factor vs applied field.	48
31	Results of cavity perturbation measurements at 9.5 GHz on a 2.0% by volume sample of SF Special carbonyl iron powder in epoxy: (a) frequency shift vs applied magnetic field; and (b) reciprocal of the sample Q-factor vs applied field.	50



LIST OF FIGURES

<u>Figure</u>		<u>Page</u>
32	Results of cavity perturbation measurements at 9.5 GHz on a 2.0% by volume sample of EW carbonyl iron powder in epoxy: (a) frequency shift vs applied magnetic field; and (b) reciprocal of the sample Q-factor vs applied field.	51
33	Results of cavity perturbation measurements at 9.5 GHz on a 2.0% by volume sample of carbonyl iron powder W in epoxy: (a) frequency shift vs applied magnetic field; and (b) reciprocal of the sample Q-factor vs applied field.	52
34	Results of cavity perturbation measurements at 9.5 GHz on a 2.0% by volume sample of carbonyl iron powder KX in epoxy: (a) frequency shift vs applied magnetic field; and (b) reciprocal of the sample Q-factor vs applied field.	53
35	Magnetization of approximately 40% by volume of carbonyl iron in a polymeric matrix of about $0.6 \times 1.2 \times 0.055$ cm: (a) magnetization vs applied field for the sample oriented parallel to the applied field; and (b) magnetization vs applied field or the sample oriented perpendicular to the applied field.	56

LIST OF TABLES

<u>Table</u>		<u>Page</u>
1	NIST Magnetic Units	4
2	Properties of Carbonyl Iron Samples Used in This Program	18



1.0 OBJECTIVE

The objective of this program was to gather information to formulate a microwave absorber that can work in the presence of strong constant (DC) magnetic fields.

The program was conducted in four steps. The first step was to investigate the electrical and magnetic properties of magnetic and ferrite microwave absorbers in the presence of strong magnetic fields. This included both experimental measurements and a literature survey of properties that may be applicable to finding an appropriate absorbing material. The second step was to identify those material properties that will produce desirable absorptive properties in the presence of intense magnetic fields and determine the range of magnetic field in which the absorbers remain effective. The third step was to establish ferrite absorber designs that will produce low reflection and adequate absorption in the presence of intense inhomogeneous static magnetic fields. The final step was to prepare and test samples of such magnetic microwave absorbers if such designs seem practical.



2.0 INTRODUCTION

2.1 Magnetic Units and Terminology

There is a great deal of confusion concerning magnetic units and terminology. Three systems of units frequently used are cm-g-s (cgs) system, electromagnetic units (emu), and System Internationale (SI). These are described briefly below. The preferred system of units is SI. However, most of the relevant magnetic parameters for materials currently available are expressed in the emu system. More thorough coverage of magnetic units can be found in any of the general texts listed in the bibliography (Appendix 1). The cgs system is closely related to the emu system.

For the purposes of this report, the emu system will be used. In this case, the magnetic field, H , is expressed in Oersted (Oe), the magnetic flux density, B , in Gauss (G), and the magnetization of a material, M , in electromagnetic units (emu). The relationship between these parameters is given in Eq. 1,

$$\mathbf{B} = \mathbf{H} + 4\pi\mathbf{M} \quad (1)$$

where the bold font indicates a vector quantity. The magnetic permeability of a material, μ , is the ratio of B to H , so that

$$\mu = 1 + 4\pi\mathbf{M}/H = 1 + 4\pi\chi \quad (2)$$

where χ is the magnetic susceptibility, \mathbf{M}/H . It is easy to see that $\mathbf{B} = \mu\mathbf{H}$. In fact, μ is a tensor, but for the purposes of this report it will be considered as a scalar.

In SI units, both H and M are given in Amperes/m (A/m) and B in Tesla (T). The relationship between B , H , and M is

$$\mathbf{B} = \mu_0 (\mathbf{H} + \mathbf{M}) \quad (3)$$

where $\mu_0 = 4\pi \times 10^{-7}$ Henries/m. The permeability is still the ratio of B to H ,



$$\mu = \mu_0(1 + M/H) \quad (4)$$

To make this dimensionless, the relative permeability μ_R is defined as μ/μ_0 . The SI value of μ_R is numerically equivalent to the emu value of μ . The magnetic susceptibility is the ratio of M to H , which is 4π times greater than the emu value. A copy of the conversion chart prepared by the National Institute of Standards and Technology for conversion between SI and emu systems is given in Table 1.

Two additional properties of magnetic materials are important for this work. First is the magnetic saturation, M_S which is the total magnetic moment per unit volume when all of the electron spins are aligned in the same direction. The second parameter is the magnetocrystalline anisotropy, H_A . Each material exhibits an easy axis of magnetization. For example, iron has its easy axis along one edge of the cubic crystal structure, and barium ferrite has the easy axis in the plane of its hexagonal structure. The magnitude of H_A is the additional magnetic field needed to saturate the hard axis rather than the easy axis of a single crystal.

2.2 Magnetic Loop

Some of the results obtained on this program can be understood in terms of the "magnetic loop." The magnetic loop presents the magnitude of the magnetization within any material as either B or M vs. the magnitude of H . The loop is made by scanning H between saturation limits of the magnetic material. Two examples of plots of M vs H are shown in Fig. 1. Although these were recorded over relatively large applied DC fields, up to 10 kOe, one could also envision that analogous curves can be recorded at any frequency where the applied fields may be as small as a few mOe, and the closed loop represents one cycle. These small loops are called minor loops.

Figure 1(a) shows a typical M - H loop for a moderate coercivity magnetic material. The coercivity represents the magnetic field that must be applied to a material in the opposite direction of its magnetization to reduce its magnetization to zero. As examples, a permanent magnet would represent high coercivity material because it is very difficult to demagnetize, while an iron nail represents a low coercivity material because it is magnetized only in the presence of a magnetic field.



Table 1
Units for Magnetic Properties

Quantity	Symbol	Gaussian & cgs emu ^a	Conversion factor, C ^b	SI & rationalized mks ^c
Magnetic flux density, magnetic induction	B	gauss (G) ^d	10^{-4}	tesla (T), Wb/m ²
Magnetic flux	Φ	maxwell (Mx), G·cm ²	10^{-8}	weber (Wb), volt second (V·s)
Magnetic potential difference, magnetomotive force	U, F	gilbert (Gb)	$10/4\pi$	ampere (A)
Magnetic field strength, magnetizing force	H	oersted (Oe), ^e Gb/cm	$10^3/4\pi$	A/m ^f
(Volume) magnetization ^g	M	emu/cm ³ ^h	10^3	A/m
(Volume) magnetization	$4\pi M$	G	$10^3/4\pi$	A/m
Magnetic polarization, intensity of magnetization	J, I	emu/cm ³	$4\pi \times 10^{-4}$	T, Wb/m ² ⁱ
(Mass) magnetization	σ, M	emu/g	$\frac{1}{4\pi \times 10^{-7}}$	A·m ² /kg Wb·m/kg
Magnetic moment	m	emu, erg/G	10^{-3}	A·m ² , joule per tesla (J/T)
Magnetic dipole moment	j	emu, erg/G	$4\pi \times 10^{-10}$	Wb·m ⁱ
(Volume) susceptibility	χ, κ	dimensionless, emu/cm ³	$\frac{4\pi}{(4\pi)^2} \times 10^{-7}$	dimensionless henry per meter (H/m), Wb/(A·m)
(Mass) susceptibility	χ_p, κ_p	cm ³ /g, emu/g	$\frac{4\pi \times 10^{-3}}{(4\pi)^2 \times 10^{-10}}$	m ³ /kg H·m ² /kg
(Molar) susceptibility	χ_{mol}, κ_{mol}	cm ³ /mol, emu/mol	$\frac{4\pi \times 10^{-6}}{(4\pi)^2 \times 10^{-13}}$	m ³ /mol H·m ² /mol
Permeability	μ	dimensionless	$4\pi \times 10^{-7}$	H/m, Wb/(A·m)
Relative permeability ^j	μ_r	not defined		dimensionless
(Volume) energy density, energy product ^k	W	erg/cm ³	10^{-1}	J/m ³
Demagnetization factor	D, N	dimensionless	$1/4\pi$	dimensionless

- a. Gaussian units and cgs emu are the same for magnetic properties. The defining relation is $B = H + 4\pi M$.
- b. Multiply a number in Gaussian units by C to convert it to SI (e.g., $1 \text{ G} \times 10^{-4} \text{ T/G} = 10^{-4} \text{ T}$).
- c. SI (*Système International d'Unités*) has been adopted by the National Bureau of Standards. Where two conversion factors are given, the upper one is recognized under, or consistent with, SI and is based on the definition $B = \mu_0(H + M)$, where $\mu_0 = 4\pi \times 10^{-7} \text{ H/m}$. The lower one is not recognized under SI and is based on the definition $B = \mu_0 H + J$, where the symbol I is often used in place of J .
- d. 1 gauss = 10^3 gamma (γ).
- e. Both oersted and gauss are expressed as $\text{cm}^{-1/2} \cdot \text{g}^{1/2} \cdot \text{s}^{-1}$ in terms of base units.
- f. A/m was often expressed as "ampere-turn per meter" when used for magnetic field strength.
- g. Magnetic moment per unit volume.
- h. The designation "emu" is not a unit.
- i. Recognized under SI, even though based on the definition $B = \mu_0 H + J$. See footnote c.
- j. $\mu_r = \mu/\mu_0 = 1 + \chi$, all in SI. μ_r is equal to Gaussian μ .
- k. $B \cdot H$ and $\mu_0 M \cdot H$ have SI units J/m³; $M \cdot H$ and $B \cdot H/4\pi$ have Gaussian units erg/cm³.

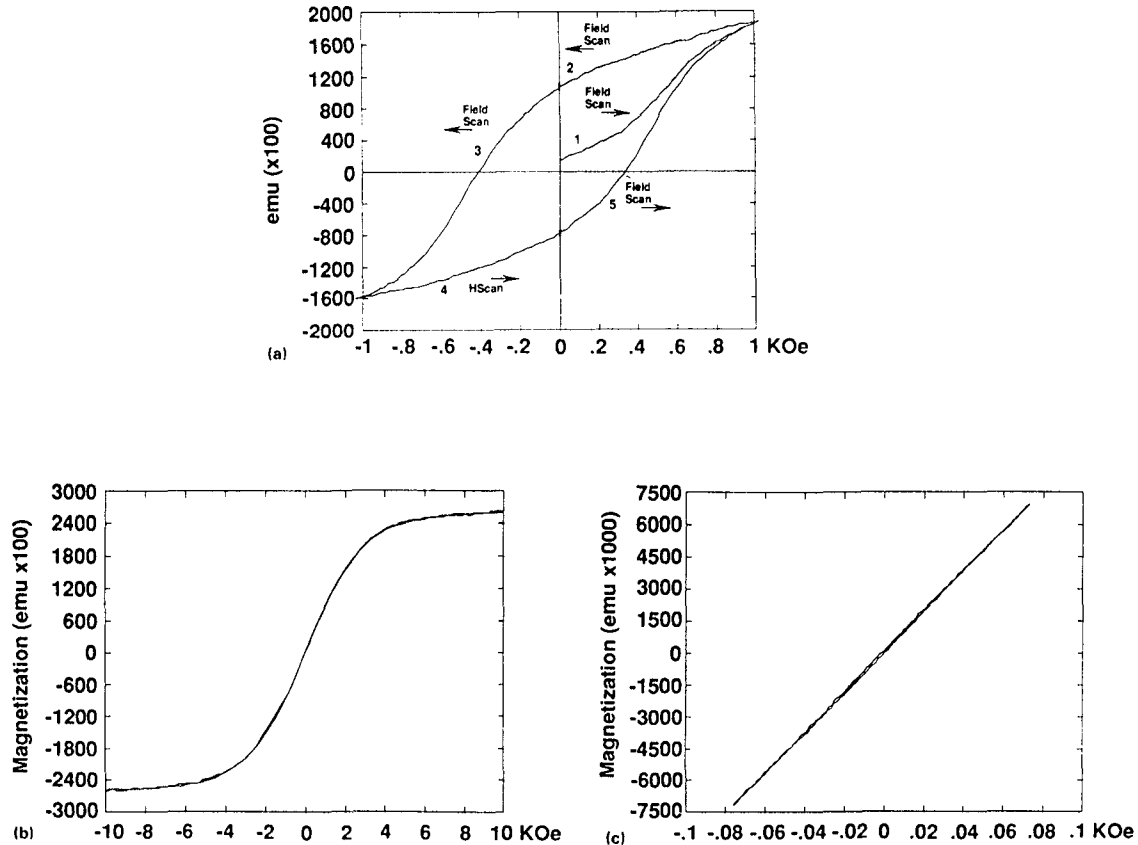


Fig. 1 M-H loops: (a) Typical moderate coercivity material; (b) Iron carbonyl powder exhibiting low coercivity (sample size approximately $1.2 \times 0.6 \times 0.055$ cm); and (c) Minor loop of b around small applied magnetic fields.

An M-H loop can be broken into five segments as indicated in Fig. 1(a): (1) The magnetic field applied to a demagnetized sample is increased from zero until the material is magnetically saturated. In this region, as the magnetic field is first increased from zero, the magnetization increases at an increasing rate. That is, the sample is more difficult to magnetize when it is fully demagnetized, than after it is slightly magnetized. As the applied field is further increased, the magnetization approaches a plateau known as saturation. (2) The magnetic field is then decreased to zero. In this region, as the magnetic field is decreased the magnetization of the sample is reduced, but there is still remanent magnetization at zero applied field. (3) The magnetic field is



SC73001.FR

reversed and scanned to the same magnitude as in step 1. At a sufficiently negative field, known as the coercive field, the magnetization is reduced to zero. As the scan is continued in the negative direction the sample again becomes magnetically saturated. (4) The field is then scanned back to zero. This traces the same curve as in step 2, but with M and H reversed. (5) The field is then scanned back in the positive direction until the sample is magnetically saturated. This portion of the loop is equivalent to step 3, but with M and H reversed.

The mechanism by which materials become magnetized is by changes in the size of the magnetic domains present in all magnetic materials. A schematic diagram of the changes in the domain structure of a magnetic material during magnetization is shown in Fig. 2. Domains are separated by a region or "wall" over which the direction of magnetization changes. When a material is completely demagnetized, its domains are the smallest region of a material that can remain magnetized, but the magnetic moments of the domains add to give zero net magnetization such as shown in Fig. 2(a). During the process of magnetization, the sizes of domains with magnetization in the direction of the applied field increase, while those with their magnetization opposite to the applied field decrease as shown in Fig. 2(b). When the material becomes magnetically saturated, all of the magnetic moments within the material align in the same direction, as shown in Fig. 2(c), and the sample is said to be single domain. The magnetic field required to achieve this condition must be greater than $4\pi M_S D$, where D is the demagnetization factor described in Sect. 2.3.

Carbonyl iron powders (CIP) dispersed in composite coatings are used extensively as microwave absorbers. The M-H loop of a typical sample of about 40% by volume in a polymeric binder is shown in Fig. 1(b). The sample size is about 10 mm x 5 mm x mm. The magnetic field was applied parallel to the plane containing the 5 mm x 10 mm face. The coercivity of this material is extremely low and could not be resolved in the scan between -10 kOe and +10 kOe (Fig. 1(b)). As a result, Sects. 1, 3, and 5 of the loop, as described above, superimpose on each other as do Sects. 2 and 4. Even reducing the applied field by a factor of 100, Fig. 1(c), shows no apparent magnetic coercivity. These data will be used to describe some of the results obtained in this program.

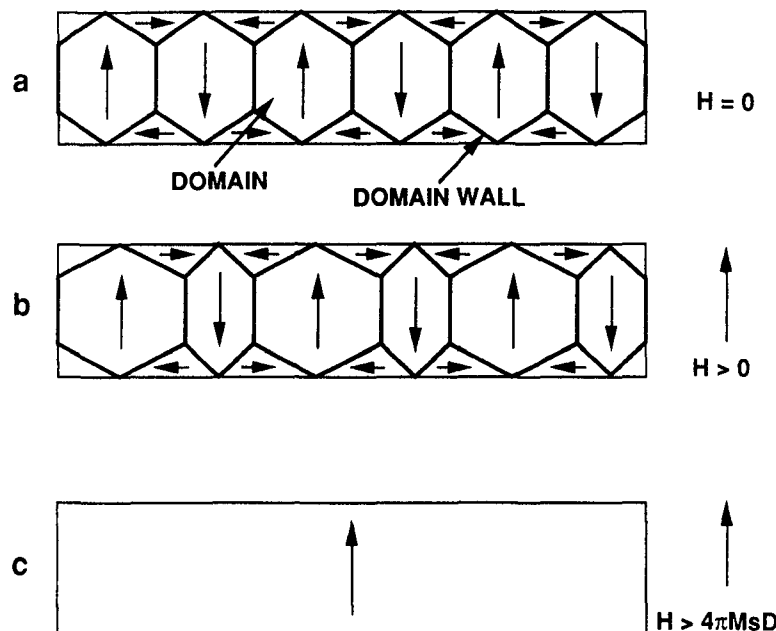


Fig. 2 Schematic representation of the domain structure of (a) nonmagnetized magnetic material; (b) partially magnetized material; and (c) fully magnetized material.

2.3 Magnetic Permeability

Measurements of the permeability of microwave absorbing materials is usually carried out in the absence of any constant magnetic field other than the 0.3-0.5 Oe due to the magnetic field of the earth. This small field is rarely of any importance, and is often neglected. It can be significant only when the DC permeability is extremely large as in the case of magnetic shielding materials. The purpose of this work is to investigate the behavior of magnetic microwave absorbing materials in the presence of fields of the order of several thousand Oe.

When measurements are made in the absence of any magnetic field other than a small perturbation that may be of any frequency or DC, the measured permeability is usually called the initial permeability. This is somewhat unfortunate because many different mechanisms can contribute to the real and imaginary parts of the permeability.



The primary mechanisms that contribute to absorption of energy by magnetic materials are:

- Hysteresis
- Eddy current losses
- Domain wall motion
- Domain rotation
- Ferromagnetic Resonance

These are in the general order of increasing frequency. The actual frequency and bandwidth of each mechanism vary among materials, so the sequence can be different from that given above. These mechanisms are well known and additional information can be found in numerous texts, including those given in Appendix I which were selected for a general review on microwave magnetics.

All of the above loss mechanisms can be described in terms of a real and an imaginary component of the magnetic permeability,

$$\mu = \mu' + i\mu'' \quad . \quad (5)$$

The real part describes the lossless part of the permeability, and at DC, where the magnetic parameters are defined such as in Eq. 1-4, there is no absorption of energy. In general, when a magnetic material is placed in an oscillating magnetic field, there may be both in-phase and out-of-phase components of permeability. The in-phase component, μ' , is proportional to the magnetic flux density in the material, and the out-of-phase component, μ'' , is related to the absorption of energy. It is simple to show that an out of phase component of magnetization will result in energy absorption.

Hysteresis loss is generally the lowest frequency loss mechanism. This results when the M-H loop exhibits significant coercivity, such as in Fig. 1(a). Because there is a phase lag of the magnetization vector with respect to the applied magnetic field, energy is required to change the magnetization of the material with respect to the applied field. Typically this mechanism is operative in the audio frequency region.



SC73001.FR

Large eddy current losses occur when electrically conductive magnetic material is placed in an oscillating magnetic field. The permeability is large enough for the field to magnetize the material (Fig. 3(a)) and cause a large internal magnetic flux density (Fig. 3(b)). In turn, the flux density induces a current in the conductive material (Fig. 3(c)). Energy is then dissipated by ohmic losses. This mechanism can be viewed qualitatively in terms of Maxwell's equation,

$$\nabla \times \mathbf{E} = 1/c \cdot d\mathbf{B}/dt \quad (6)$$

where the electric field (\mathbf{E}) generated in a material is proportional to the time dependence of the flux density within the material. Assuming μ is constant through each cycle of the field applied to the material,

$$\nabla \times \mathbf{E} = \mu/c \, d\mathbf{H}/dt \quad (7)$$

In turn, the magnitude of the current is proportional to the magnitude of the electric field, $|\mathbf{E}|$, and is inversely proportional to the resistivity, ρ , of the material,

$$i = |\mathbf{E}|/\rho \quad (8)$$

The energy dissipation per unit volume, W , is then proportional to $i^2\rho$. Combining Eqs. 7 and 8, and considering only the magnitudes of the vectors gives the power dissipation, W , in terms of the current, resistivity, and time dependent magnetic field,

$$W = i^2\rho = \mu^2/\rho c^2 \cdot (dH/dt)^2 \quad (9)$$

If the material is thicker than the skin depth of field penetration into the material, the energy losses occur only at the surface. On the other hand, if the material is thinner than the skin depth, very small current loops are induced, so that the loss is very low.

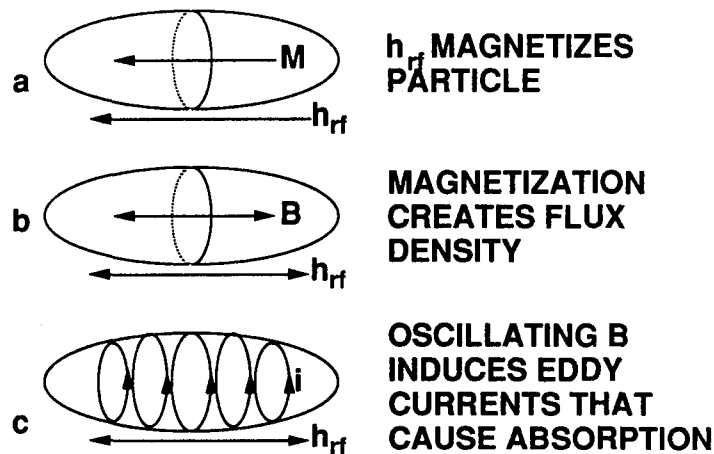


Fig. 3 Schematic drawing of the mechanism of eddy current losses due to a conductive magnetic particle in an oscillating magnetic field: (a) oscillating field induces magnetization in the particle; (b) magnetization creates internal flux density; and (c) currents are induced by the time dependent magnetic flux.

Carbonyl iron powders have diameters (1-7 μm) of similar magnitude to their skin depth in the microwave region where their permeability is still sufficiently large so that significant eddy currents are induced in the particles. As a result, these materials are used as microwave absorbers in the 2-18 GHz frequency range. If the particles were larger, the interior would be screened from the microwave magnetic field, and the loss per unit volume would decrease. On the other hand, if the particles were smaller, the current loop would be smaller also reducing the loss per unit volume.

In some circumstances energy can be dissipated by domain wall motion. In this mechanism magnetic domains synchronously increase and decrease in response to an oscillating applied magnetic field. Comparison of Figs. 2(a) and 2(b) provides an example of how such domain motion occurs. Generally, the coercivity of the material must be low, and the frequency range over which this occurs can be up to about 50 MHz. The frequency, f , at the peak of the absorption is proportional to the saturation magnetization and is inversely proportional to the low frequency permeability, μ , of the material¹

$$f(\text{MHz}) \approx 2.80 \cdot 4\pi M_S / \mu \quad (10)$$



SC73001.FR

in the absence of an applied DC magnetic field. Application of a small field may enhance the loss, but if too strong a field is applied, the loss decreases because the domain sizes become large so that the wall motion is reduced. This can be considered a resonance phenomenon in that the domain motion is synchronous with the frequency of the oscillating magnetic field. Thus, the absorption is limited to a narrow frequency, and the bandwidth is related to the response of the domains.

Domain rotation is another resonant mechanism in which the magnetization of each domain rotates in resonance with an oscillating magnetic field. The frequency, f , at the peak of the absorption of polycrystalline materials is given by²

$$f(\text{MHz}) \approx 2.8026 \cdot [(H_A + 4\pi M_S) H_A]^{1/2} \quad (11)$$

in the absence of a DC magnetic field. For a polycrystalline material the minimum absorption frequency is approximately $2.80 \cdot H_A$. The theoretical maximum frequency could be as large as $2.80 \cdot (H_A + 4\pi M_S)$, depending on the direction of the microwave field with respect to the overall geometry of the material. This upper limit is rarely realized. For example, if this were true, soft iron should exhibit domain wall resonance at frequencies as large as 60 GHz because $4\pi M_S$ is 21,000 Oe. In practice, the upper limit of this behavior is usually about 1 GHz. The maximum permeability due to this effect is given approximately by

$$\mu' \approx 1 + 2/3 \cdot (1 - p) \cdot 4\pi M_S / H_A \quad (12)$$

where p is the porosity of the material. Typically, domain rotation resonance in random materials occurs over a band of 200-500 MHz, with peak values of μ' between 10 and 1000, and peak values of μ'' between about 8 and 500. An example of a microwave absorber based on this phenomenon is the Emerson-Cuming NZ series ferrite tiles.

Usually domain rotation is measured in the absence of a magnetic field. Application of a large magnetic field changes the domain structure, so that the magnitude changes as the applied field is increased, and disappears when the material is



SC73001.FR

magnetically saturated. The applied field will also bias the resonance frequency toward larger values.

Ferromagnetic resonance^{1,3} is similar to domain rotation, except in this case the spin of unpaired electrons "flip" direction to cause absorption of energy. Generally this phenomenon is best observed when the material is magnetically saturated. Thus, for single domain particles, resonances can be observed with no applied field, but for bulk materials, the effect is best observed when large applied fields are used. The magnetic field will bias the resonance by about 2.80 MHz/Oe. The resonant field is therefore a function of the saturation magnetization and anisotropy field of the material, the particle geometry of the sample, and of the applied magnetic field. In general the bandwidth is no more than several hundred MHz.

For any sample, the geometry will have an effect on the measured permeability even though the intrinsic permeability is not affected. This effect occurs through demagnetization fields. When a discontinuous material is magnetized, magnetic poles form at the surface. These poles exert a magnetic field in the sample that opposes the applied field. This secondary field is known as the demagnetization field. Thus, in emu units, the flux density within the sample is given by

$$B = H + 4\pi M(1-D) \quad (13)$$

where D is known as the demagnetization factor. The value of D is geometry dependent, and all of the components add to unity. For example, for a sphere, the demagnetization factor for magnetization in each direction is 1/3. For an infinitely long rod, the value of D along the axis is zero because the poles are infinitely far apart, but the value for D in each direction perpendicular to the axis is 1/2. For an infinitely long thin sheet, D is zero when the magnetic field is in the plane and 1 when it is normal to the plane. For finite sized materials, D is constant only for a uniformly magnetized ellipsoid. Any other sample geometry is only approximately described by a constant value. If a constant value is assumed, then the measured permeability, μ_m , is given by



$$\mu_m = \mu / [1 + D(\mu - 1)] \quad . \quad (14)$$

Thus, the effective permeability approaches $1/D$ for the most magnetic material.

When a composite matrix of magnetic particles, such as spherical carbonyl iron particles, in a polymer is made, the magnetic properties of the matrix differ from those of the individual particles. If an exact equation that represents the matrix in terms of the permeability of the magnetic constituent were known, then the demagnetization could be interpreted in terms of the overall geometry of the composite. However, such "mixing" equations are not known. As a result, the demagnetization must be viewed as deviating from that of the individual particles. For example, when the composite is dilute in the magnetic component, i.e. less than about 5% by volume, it essentially exhibits the demagnetization of the individual particles. However, as the particles become more concentrated, the overall shape of the composite structure increases its influence on the demagnetization. Thus, the effect of particle concentration on the microwave absorbing properties should be examined.



3.0 RESULTS AND DISCUSSION

3.1 Concept for Preliminary Test

To obtain a good microwave absorber over a wide magnetic field, high microwave magnetic permeability over the necessary field range must be obtained. Based on the above analysis, the most logical candidate material for a magnetic microwave absorber that will function in the presence of a strong DC magnetic field and also exhibit broad bandwidth are carbonyl iron powders (CIP). Absorption occurs by the nonresonant eddy current loss mechanism which is inherently broad band. If the applied (DC) magnetic field is not so strong as to magnetically saturate the material, μ can remain sufficiently large so that a weak applied oscillating field can cause internal fields large enough to induce electric current in the particle. Furthermore, the DC magnetic field should not shift the absorption. Because the particles are spherical, the minimum field needed to reach saturation is $4\pi M_S/3$. For iron, M_S is 21 kOe. Thus, to a first approximation, carbonyl iron microwave absorbers would be expected to be effective at fields to nearly 7 kOe. Domain resonance and wall motion generally occur at frequencies that are too low to satisfy this objective, and the absorption frequency would be shifted and the effect diminished by a DC magnetic field. Ferromagnetic resonance is usually relatively narrow band and is also shifted by the DC magnetic field.

3.2 Experimental Methods

In all measurements a 15" pole diameter Magnion (now O.S. Walker) electro-magnet was used. The pole pieces were tapered to a 12" face diameter with a 3" gap for the sample cell. The power supply is capable of generating 22.5 kW (100 V, 225 A). In this configuration, the magnet is capable of a maximum field of 18.6 kOe.

3.2.1 Transmission Line Measurements

Two types of experimental measurements were used. The first was to determine the permittivity and permeability of each material as a function of frequency at different magnetic fields up to 10-15 kOe. This was carried out by placing a torroid sample in a 7 mm coaxial transmission line cell as shown in Fig. 4(a). The amplitude and



phase of the transmitted and reflected microwave signal were used to compute to real and imaginary components of permittivity and permeability (ϵ' , ϵ'' , μ' , μ'') according to the methods of Larson⁴ and others^{5,6}. These measurements were carried out with a Hewlett Packard Model 8510B Automatic Vector Network Analyzer with a dedicated Hewlett Packard Model 310 computer. Software was developed in this laboratory for conversion of the phase and amplitude data to permeability and permittivity. The TEM transmission cell used for these measurements was made to connect directly to precision APC-7 connectors. The cell length was 50.77 mm. The inside diameter of the transmission line was 7.000 mm, and the outside diameter of the coaxial conductor was 3.040 mm, resulting in a 50.00 Ω transmission line. Torroidal samples were machined to the respective inside and outside diameters with allowable tolerances of ± 0.003 mm. Sample thicknesses ranged from 1 to 4 mm. A diagram of the sample is shown in Fig. 4(b). The sample cell was placed in a uniform magnetic field with the direction indicated by the arrows in Figs. 4(a) and 4(c). Values of permeability were measured at 0, 50, 100, 250, 500, 1000, 2500, 5000, 7500, 10000, and 12500 Oe applied fields. Other fields were used for the measurement as needed. The measurements are valid up to 20 GHz, but are plotted between 1 and 21 GHz for convenience in reading the data.

In the absence of an applied magnetic field, the magnetization of the sample is affected only by the field, h , generated by the microwave power in the coaxial transmission line. This field is annular and coaxial with the cable as shown by the arrows and circles in Fig. 4(c). When the uniform magnetic field, H , is applied to the sample, the constant direction of the magnetic field destroys the magnetic cylindrical symmetry. First, if the sample is not magnetically saturated, the sample magnetization becomes inhomogeneous because the magnetization created by the applied field in turn creates magnetic poles on the inner and outer sample edges as shown by + and - in Fig. 4(c). This pole density will vary along the sample surface and create inhomogeneous demagnetizing fields. [See references in Appendix 1.] In general, M is in the same direction as the applied field, but it tends to curve around the center hole. Another effect of the applied field is that the microwave field, h , changes from perpendicular to parallel with respect to H as h transverses $1/4$ of the torroid. This is indicated by the arrows in Fig. 4(c). As a result, the angles between M and h are different throughout the sample. Since magnetic fields change gradually in space, the situation represented by the transmission line cell is

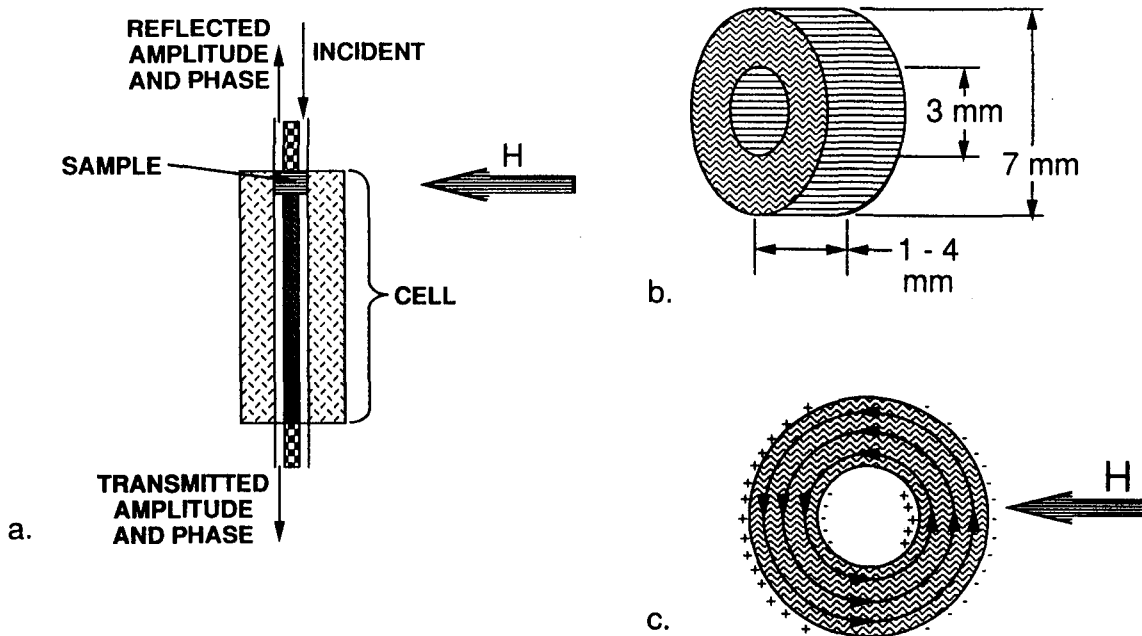


Fig. 4 (a) Diagram of 7 mm coaxial transmission line cell and direction of the applied magnetic field; (b) Torroidal sample and dimensions; and (c) diagram of the applied magnetic field and the poles generated at the sample surface.

probably representative of any realistic magnetic microwave absorbing material placed in a magnetic field. That is, the change in the polarization direction can occur over a smaller spatial region than a change in magnetic field intensity. Such an example is two faces at right angles where one face is parallel and the other is perpendicular to the microwave magnetic field.

3.2.2 Cavity Perturbation Measurements

The transmission line cell is relatively insensitive so that permeabilities and permittivities of samples with carbonyl iron concentrations smaller than about 10% by volume are difficult to measure. As a result, cavity perturbation measurements were carried out to determine the effect of magnetic field on the permeability. This measurement was done at 9.5 GHz using TE_{011} mode cavity. Both the frequency shift and change in the Q-factor were measured as a function of applied magnetic field. The cavity dimensions were 48.55 mm diameter and 24.50 mm height. In this cavity, the



magnetic field is greatest along the axis of the cavity. Therefore rod shaped samples, approximately 1.9 mm diameter were placed on the cavity axis, and made so that the sample extended through the cavity. In this experiment h and H are always perpendicular. Determination of the cavity Q and frequency shift were done "on-line" as was the above transmission line measurements. Permeability values were not determined. Rather, the parameter of interest was to find the magnetic field at which deviations in μ' or μ'' began to occur. In this case, changes of the resonant frequency and the change in the cavity Q factor from the values at zero applied magnetic field are respectively related to changes in μ' and μ'' as indicated by Eqs. 15 and 16.

$$\mu' \propto (f_0 - f)/f_0 \quad (15)$$

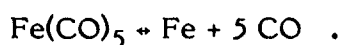
$$\mu'' \propto (1/Q - 1/Q_0) \quad (16)$$

where f_0 and Q_0 are, respectively, the frequency and Q -factors of the cavity containing an epoxy-filled sample tube; and f and Q are the frequency and Q factor of the cavity containing the sample, each at the respective applied magnetic field. The measured frequency- and Q -changes need to be corrected for a small magnetic field dependence on the empty cavity Q -factor and resonant frequency due to magnetostrictive effects. For convenience the frequency shift can be defined as $(f_0 - f)$ so that the value is always positive for positive μ' and the Q -factor of the sample can be defined as

$$1/Q_S = 1/Q - 1/Q_0 \quad (17)$$

3.2.3 Materials and Concentrations

A wide variety of carbonyl iron samples was used in these measurements. A list of the specific materials and some of their properties are given in Table 2. Most materials were obtained as a direct product from the gas phase thermal decomposition of iron pentacarbonyl,





SC73001.FR

The iron forms spherical particles that contain about 0.7% carbon. In addition, ammonia is included as a catalyst so that the particles also contain a similar amount of nitrogen. Different grades of this material are derived from crude size separations.

Table 2
Properties of Carbonyl Iron Samples Used in Program

Material	Mfgr	Powder Type	Mean Diameter (μm)	Volume Diameter (μm)	Density (g/cm^3)	Carbon (%)	Nitrogen (%)
HFQ	BASF	finest normal	1.119	1.168	7.25	0.74	0.85
EW	BASF	normal	≈ 2.5				
SF Special	GAF	finest normal	1.163	1.643	7.73	0.63	0.68
SF	GAF	normal	1.218	1.824	7.54	0.87	0.89
TH	GAF	normal	1.047	1.671	7.61	0.67	0.60
E	GAF	normal	1.425	2.501	7.51	0.65	0.91
KX	GAF	largest normal	3.320	4.474	7.66	0.86	0.84
W	GAF	nitrided	≈ 3 .		7.05	0.68	3.62
GS6	GAF	hydrogen reduced	≈ 4 .		7.86	0.10	0.00
60730-01	GAF (E)	normal	1.679	2.624	7.77	0.62	0.63
60730-05	(a)	size separated	1.168	1.950	7.54	0.76	0.71
60730-08	(a)	size separated	1.257	1.888	7.70		
60730-13	(a)	size separated	1.166	1.839	7.58		

a. Size separated fractions from sample 60730-01

The BASF and GAF samples are listed in order of increasing anticipated mean diameter. However, the variation among samples is enough that the mean sizes of different products overlap. Both size measurements and composition of the material was determined under Rockwell IR&D for another purpose. The largest size fraction is KX grade. Whereas most of the grades consist of spherical or nearly spherical powders, most of the KX material exhibits nodules on the surface, some of which are nearly as large as the main particle.

To eliminate both carbon and nitrogen, CIP can be annealed in hydrogen. An example of this material is GS6 which is extremely high purity iron. We found in other research that because the grain structure is substantially different the permeability is lower than those of the untreated products. Finally, normal CIP material can be reacted first with hydrogen then with nitrogen. The nitriding process hardens the material; an



example of this material is W. Neither the annealed nor the nitrided material is available in size fractions as small as the normal powder.

Another material, a sample of GAF type E CIP, was size separated for another program. Several small samples of remaining material were used in this study to examine the effect of particle size from a single batch of material. These samples are described in Table 2 under the 60730 series.

Concentrations of 1 to 40% CIP by volume in RTV or epoxy were prepared for test as described above. Typically the practical percolation threshold is about 50% by volume CIP. However at concentrations above 40% by volume the powder is difficult to mix uniformly throughout the composite, and the composite becomes brittle and difficult to machine. Therefore, except for special cases we have limited the concentration to 40% by volume.

3.3 Measurement Results

3.3.1 Transmission Line Measurements

Results of the measurements of 10 to 40% by volume of carbonyl iron powders dispersed in an Epoxy matrix are shown in Figs. 5-13. Figure 5 shows the permeability determined for the empty cell measured in the absence of a magnetic field and at 12.5 kOe. As anticipated, $\mu' = 1$ and $\mu'' = 0$. The "glitches" that appear in the chart result from an error in the phase angle as the phase switches from $+180^\circ$ to -180° , and is broadened by an averaging process. This could be corrected by software, but it is not so significant when the permeability is large. Similar data were obtained for the permittivity. These results, as well as other data taken at intermediate fields, show that there is no effect on the cell due to the magnetic field.

Figure 6 shows the permeability and permittivity of a 40% by volume concentration of HFQ powder in epoxy. Between fields of 0 and 2500 Oe, at frequencies between 1 and 3 GHz, μ' decreases, and between 1 and 6 GHz, μ'' decreases. However, over the same magnetic field range at frequencies between 3 and 16 GHz, μ' increases, and between 6 and 20 GHz, μ'' increases. Above about 3000 Oe, both μ' and μ'' decrease. At the fields of 5000 and 10000 Oe shown in Fig. 6(a) and 6(b), apparent resonances



SC63305

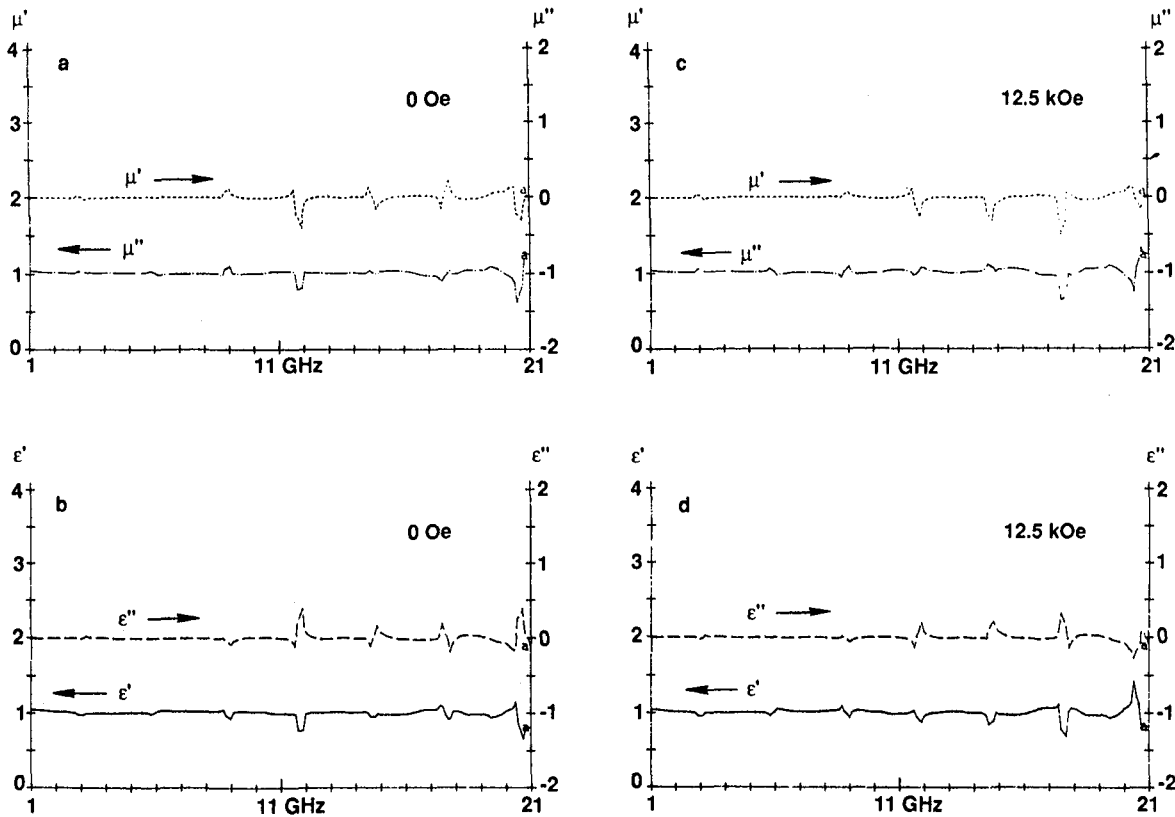


Fig. 5 Plots of the real and imaginary parts of permeability determined on the empty transmission line cell as a function of frequency at: (a) 0 Oe; and (b) 12.5 kOe.

appear between 9 and 13 GHz. Another resonance may appear at about 17-19 GHz at 10000 Oe. Because of the magnetic asymmetry of the sample, distinct ferromagnetic resonances are difficult to anticipate. Rather, a low level ferromagnetic resonance would have been expected to appear through all data.

In general the permittivity was constant over the magnetic field range tested. Typical values of ϵ' were 13-15 for 40% by volume, and 7-8 for 20% by volume. Values for ϵ'' were approximately zero, but there is a large degree of scatter in these values. A typical example of the measured field dependence of ϵ is shown in 40% by volume HFQ powder, Figs. 6(c) and 6(d). The resonances that appear in the permeability



SC73001.FR

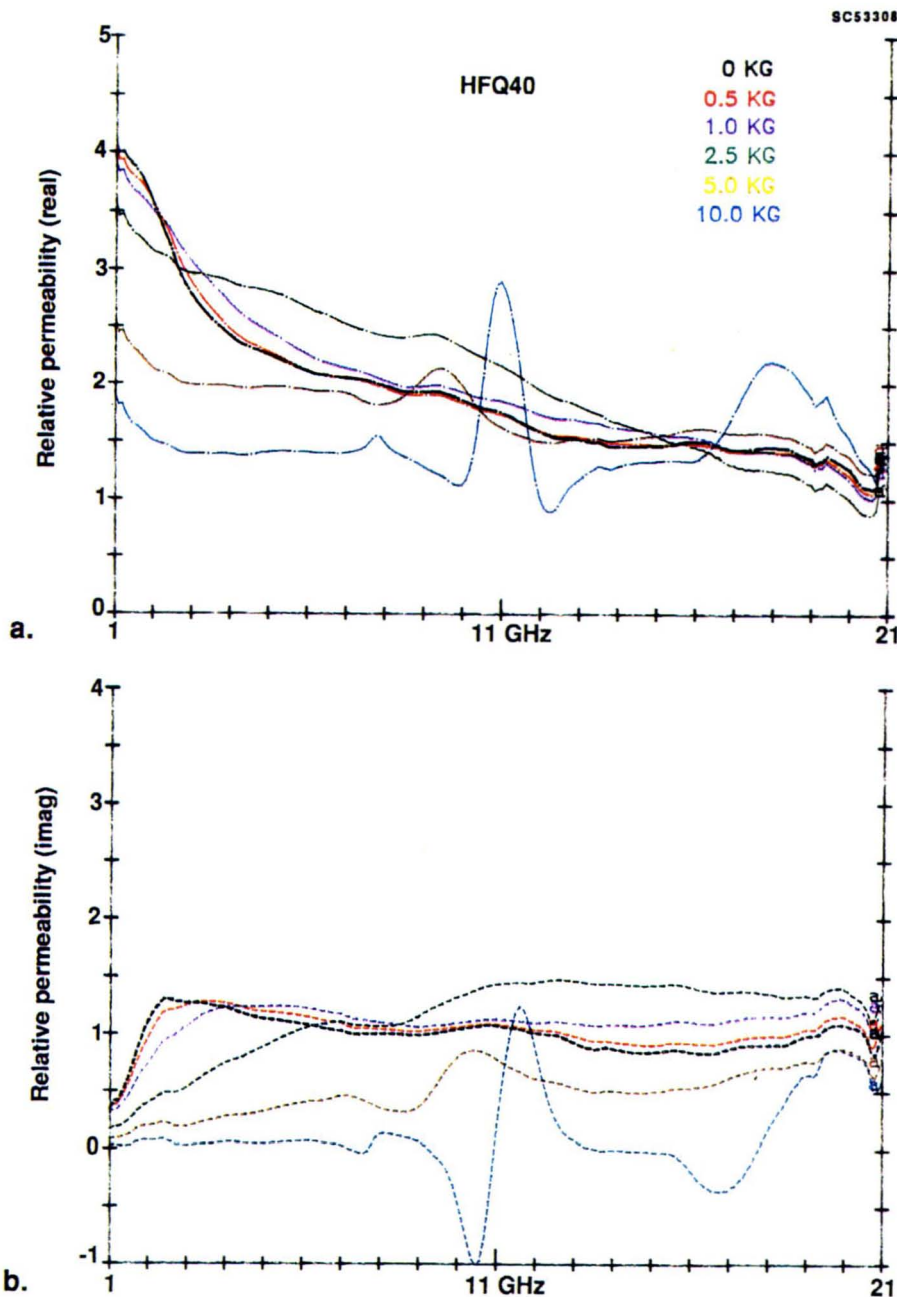


Fig. 6 Plots of the real and imaginary parts of permeability and permittivity, respectively μ' , μ'' , ϵ' and ϵ'' vs frequency (GHz) for a mixture of 40% by volume HFQ grade carbonyl iron powder in epoxy at different applied magnetic fields: (a) real part of permeability, (b) imaginary part of permeability; (c) real part of permittivity; and (d) imaginary part of permittivity.



SC73001.FR

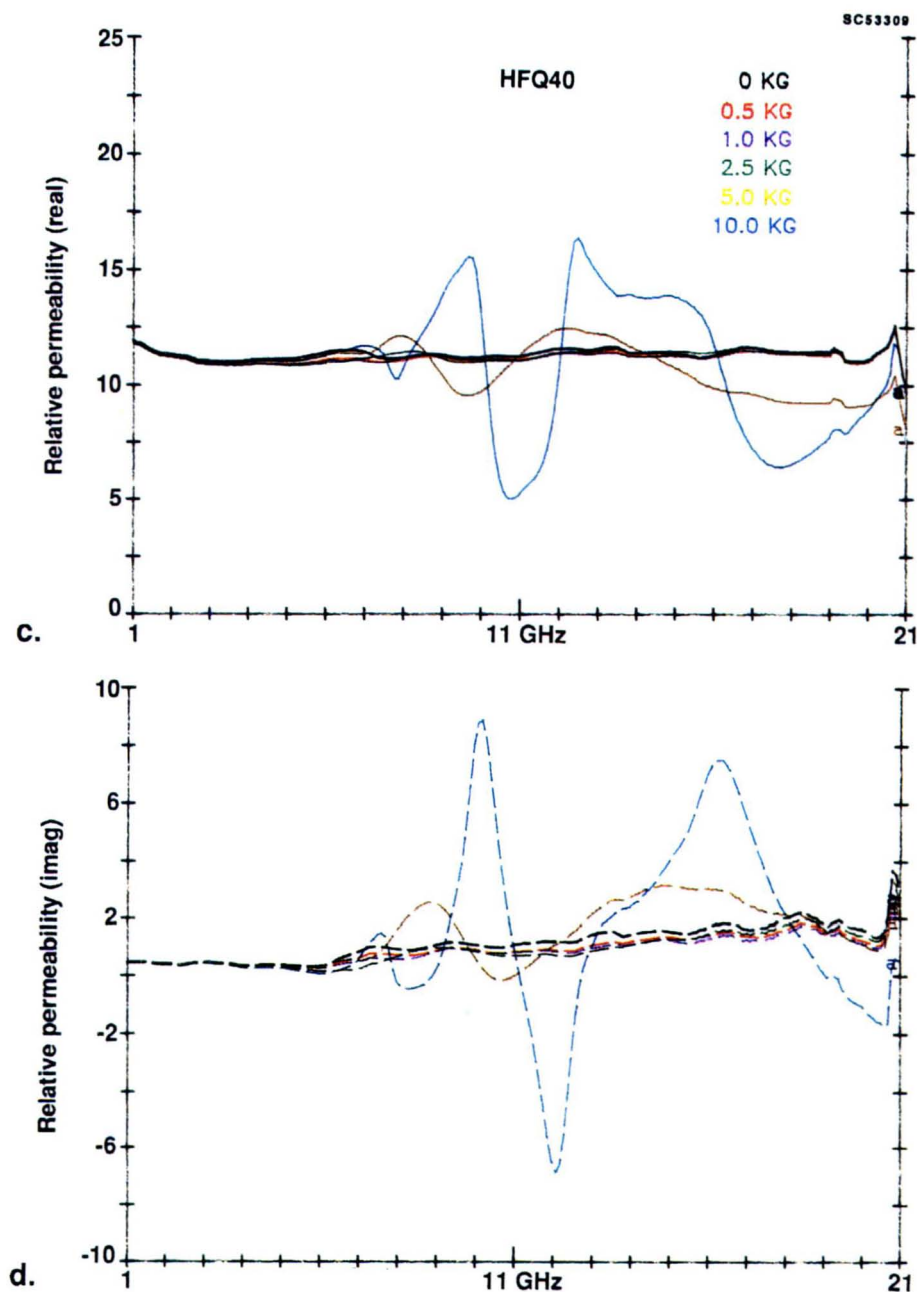


Fig. 6 (continued)



SC73001.FR

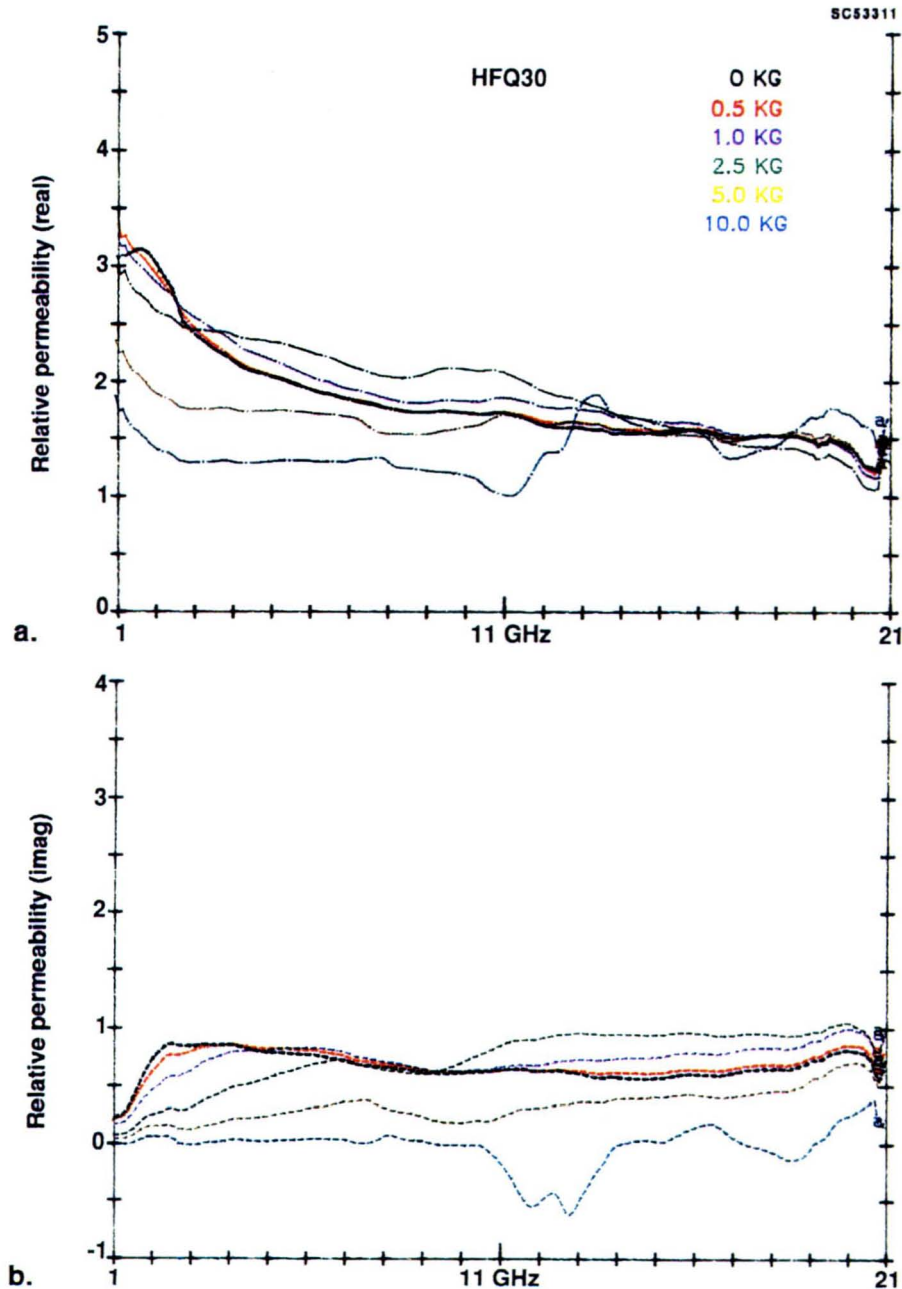


Fig. 7 Plots of the real and imaginary parts of permeability, respectively μ' and μ'' , vs frequency (GHz) for a mixture of 30% by volume HFQ grade carbonyl iron powder in epoxy at different applied magnetic fields: (a) real part of permeability and (b) imaginary part of permeability.



SC73001.FR

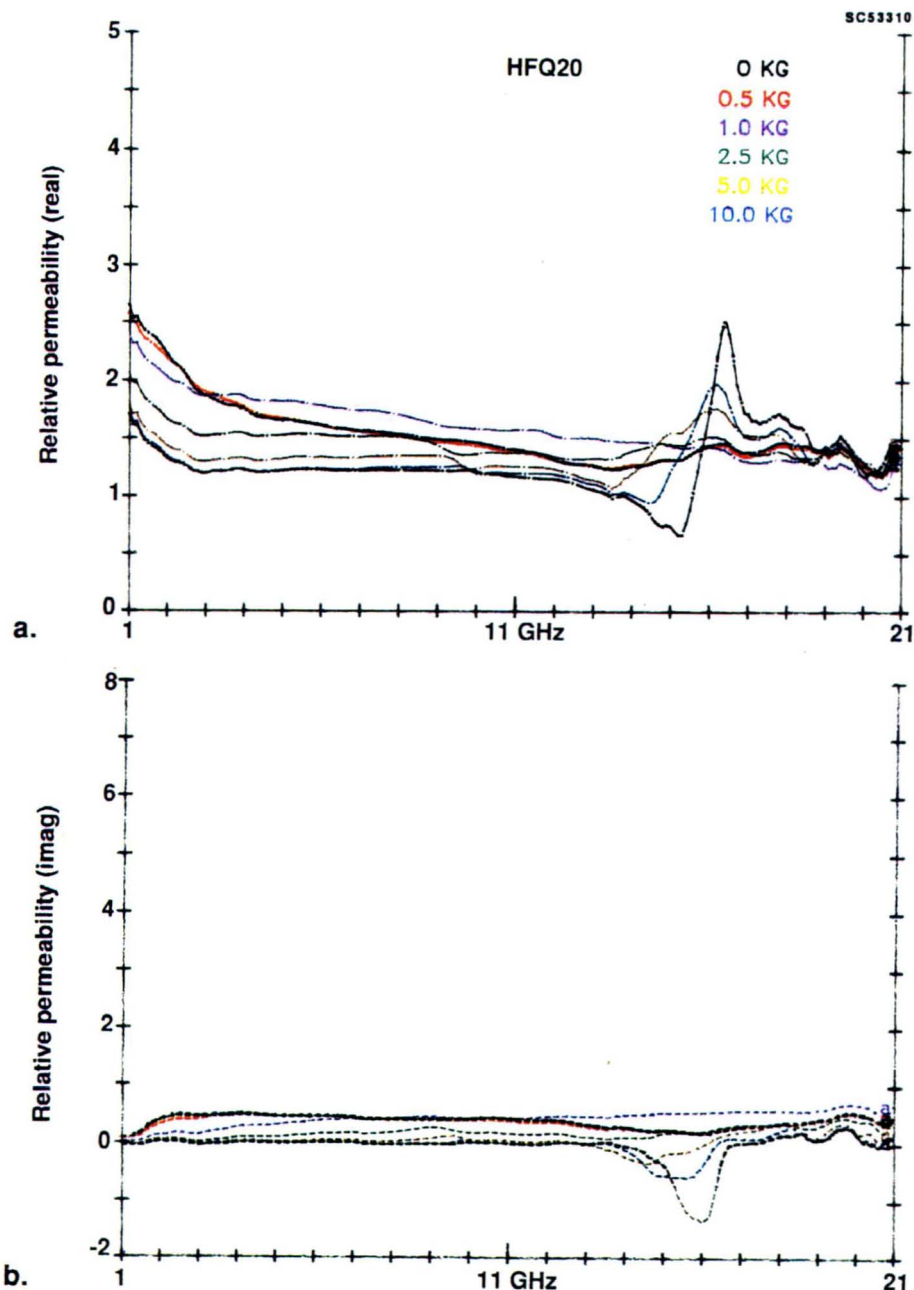


Fig. 8 Plots of the real and imaginary parts of permeability, respectively μ' and μ'' , vs frequency (GHz) for a mixture of 20% by volume HFQ grade carbonyl iron powder in epoxy at different applied magnetic fields: (a) real part of permeability and (b) imaginary part of permeability.



SC73001.FR

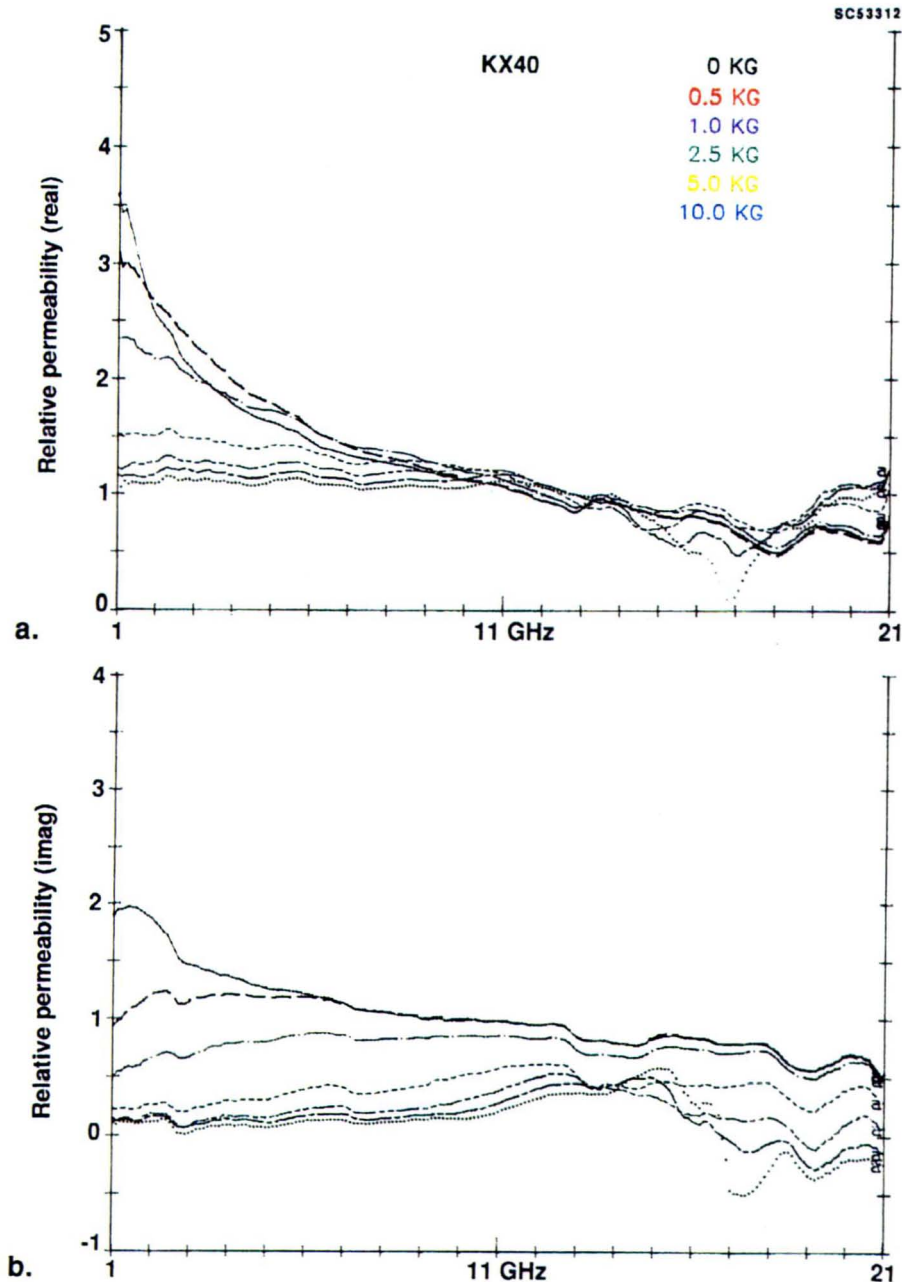


Fig. 9 Plots of the real and imaginary parts of permeability, respectively μ' and μ'' , vs frequency (GHz) for a mixture of 40% by volume KX grade carbonyl iron powder in epoxy at different applied magnetic fields: (a) real part of permeability and (b) imaginary part of permeability.



SC73001.FR

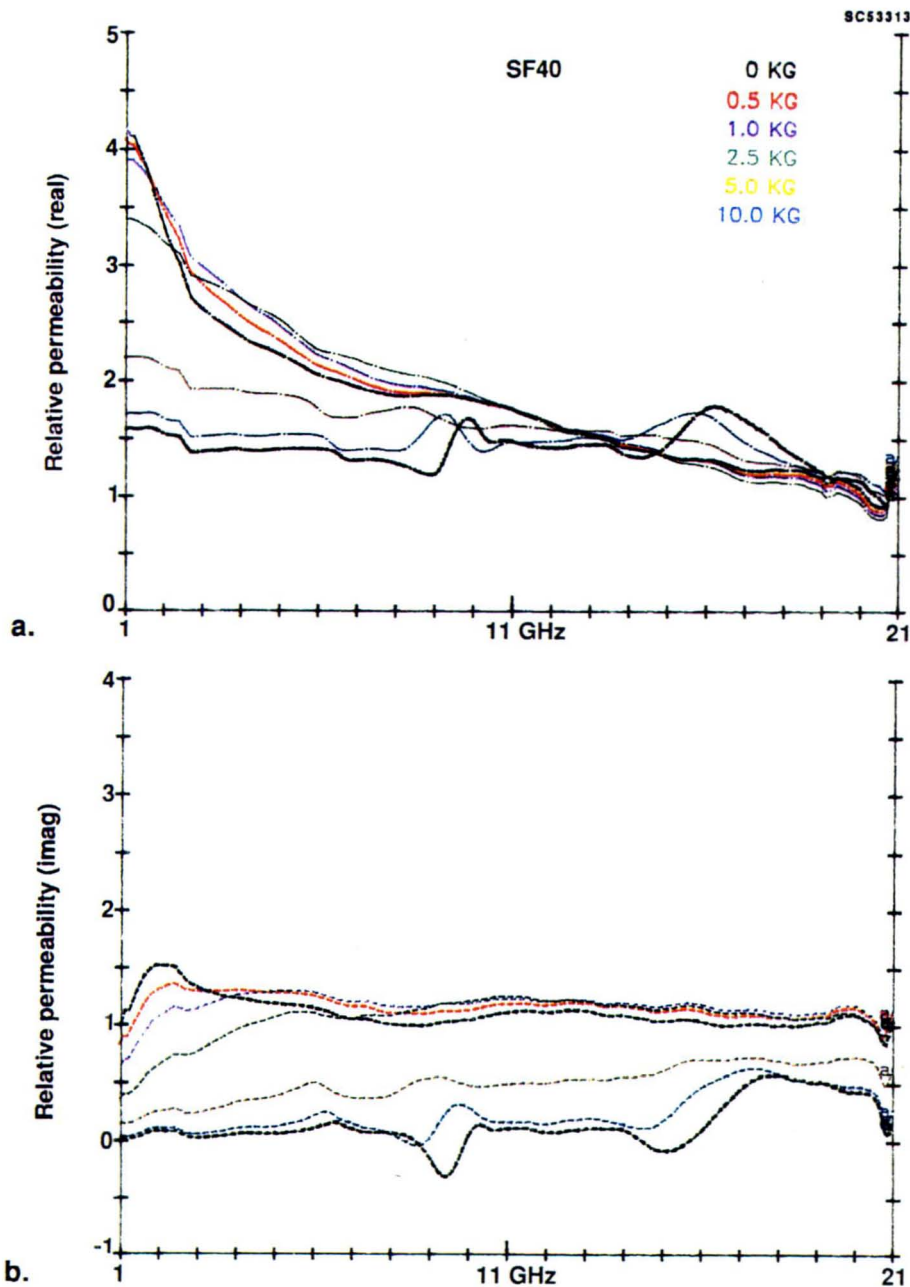


Fig. 10 Plots of the real and imaginary parts of permeability, respectively μ' and μ'' , vs frequency (GHz) for a mixture of 40% by volume SF grade carbonyl iron powder in epoxy at different applied magnetic fields: (a) real part of permeability and (b) imaginary part of permeability.



SC73001.FR

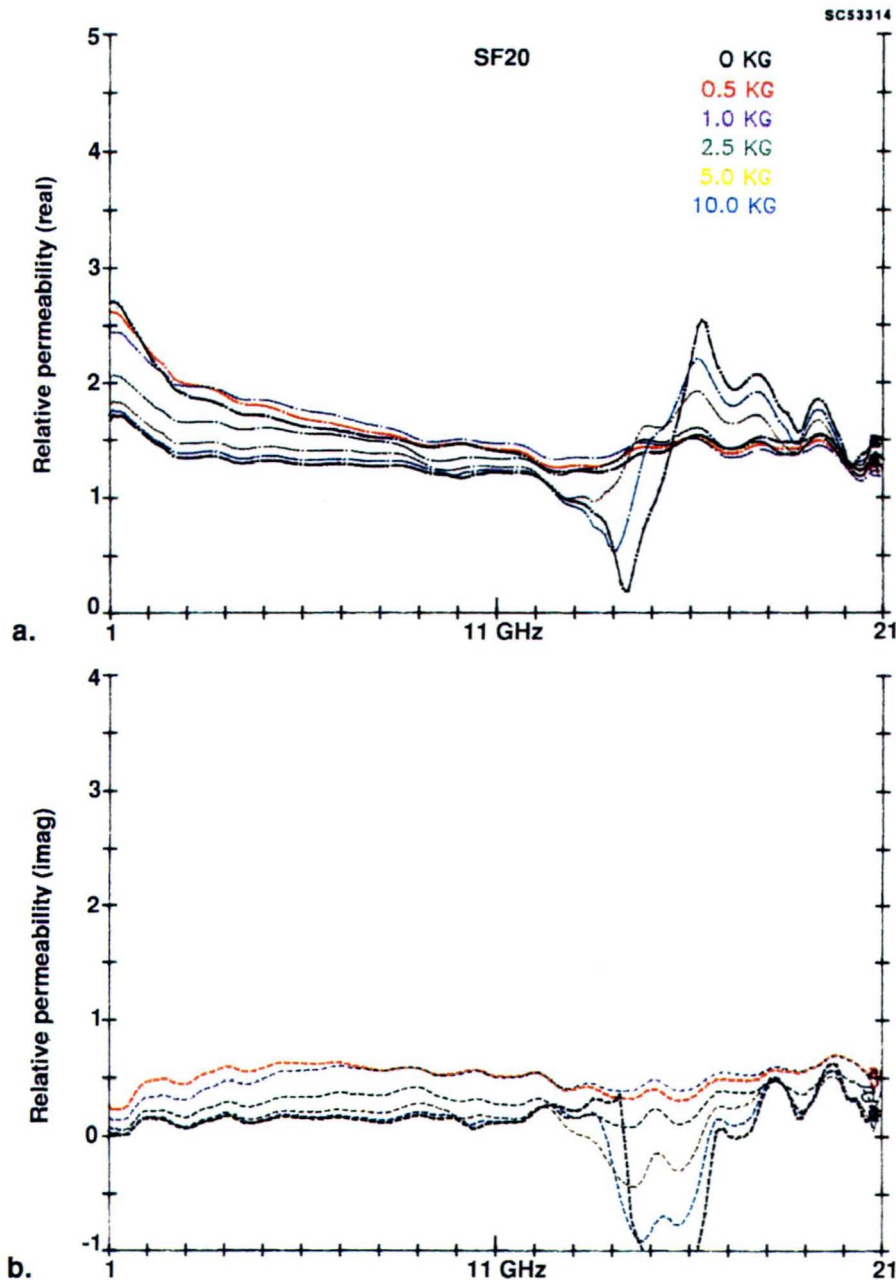


Fig. 11 Plots of the real and imaginary parts of permeability, respectively μ' and μ'' , vs frequency (GHz) for a mixture of 20% by volume SF grade carbonyl iron powder in epoxy at different applied magnetic fields: (a) real part of permeability and (b) imaginary part of permeability.



SC73001.FR

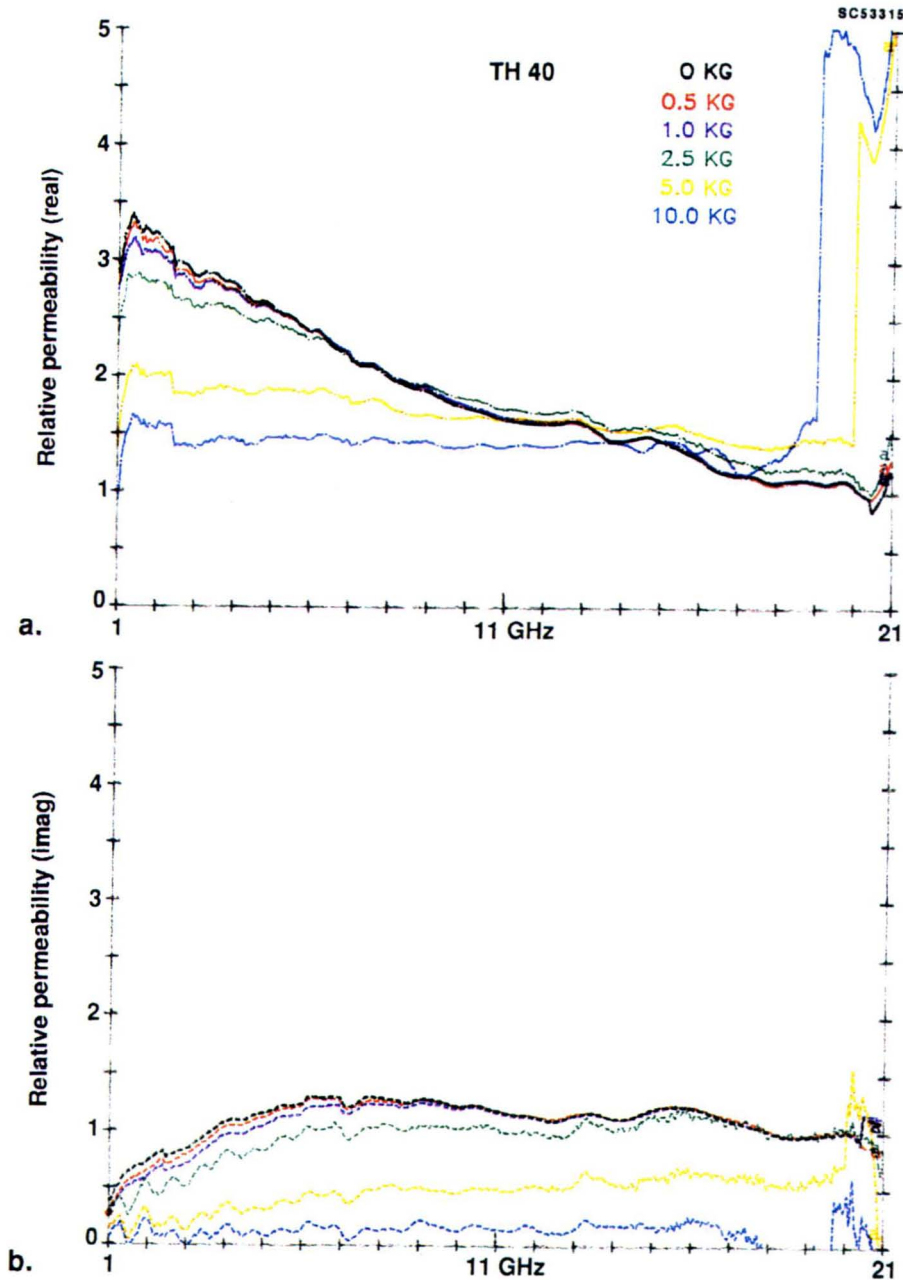


Fig. 12 Plots of the real and imaginary parts of permeability, respectively μ' and μ'' , vs frequency (GHz) for a mixture of 40% by volume TH grade carbonyl iron powder in epoxy at different applied magnetic fields: (a) real part of permeability and (b) imaginary part of permeability.



SC73001.FR

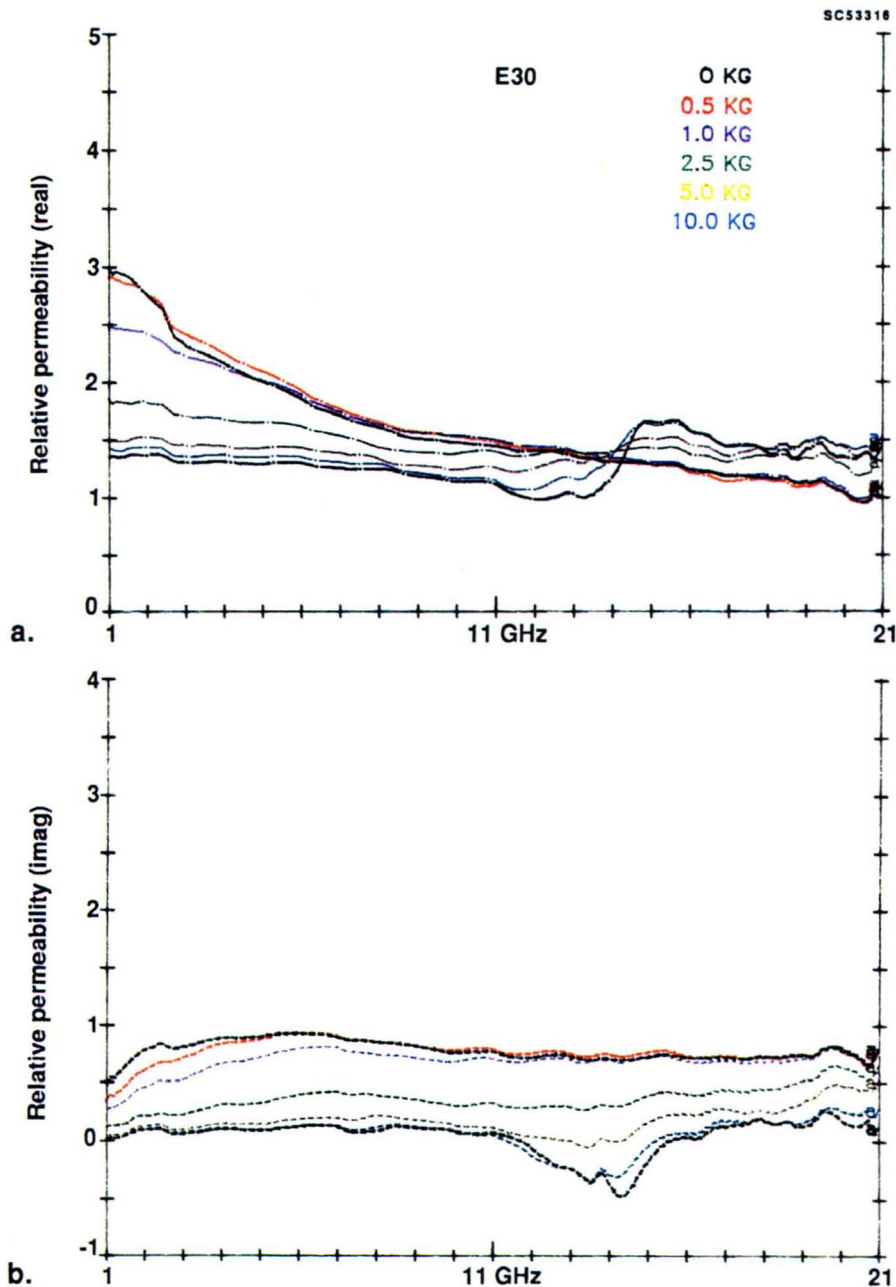


Fig. 13 Plots of the real and imaginary parts of permeability, respectively μ' and μ'' , vs frequency (GHz) for a mixture of 30% by volume E grade carbonyl iron powder in epoxy at different applied magnetic fields: (a) real part of permeability and (b) imaginary part of permeability.



SC73001.FR

with greater than 5000 Oe can also be seen in the permittivity. This was not anticipated. A tentative explanation is that with a strong applied magnetic field and the annular microwave magnetic field, resonance causes such an inhomogeneous magnetic environment that the measured amplitude and phase cannot be assigned to only the sample faces.

Values of μ' and μ'' for 30% and 20 % by volume HFQ powder are shown in Figs. 7 and 8 at various magnetic fields. The trends that are observed for the sample containing 40% by volume are followed at the lower concentrations. However, the lower concentrations cause proportionately smaller changes in permeability. The resonances observed appear to be shifted to greater frequency as the concentration is decreased.

Values of μ' and μ'' of the KX sample (Fig. 9) decrease more rapidly with frequency in the absence of an applied magnetic field than other samples tested. Thus, such material would not provide the broad bandwidth that is desirable for such material. However, this material was tested because even if it is not so effective an absorber as other materials, if the permeability did not change rapidly with field, it would still be useful because field dependent corrections would not be needed. However, magnetic field intensity did have the greatest effect on this material.

Permeability data for SF powder at 40% and 20% by volume are shown in Figs. 10 and 11 at various magnetic fields. However, in this material there is relatively little change in μ' at fields below 2500 Oe. Between 1 and 4 GHz, however, there is a relatively small decrease in μ'' over this field range. At applied magnetic fields greater than about 3000 Oe to about 5000 Oe, both μ' and μ'' decrease significantly. Above 5000 Oe, where the iron is magnetically saturated, μ' and μ'' approach, respectively 1 and 0. This differs from HFQ powder where even at 10000 Oe, the sample is not magnetically saturated. At fields above 5000 Oe resonances similar to those described above also occur.

TH type CIP, shown in Fig. 12, and Type E, shown in Figs. 13 and 14, are expected to be similar to each other. These are also magnetically similar to the SF powder.



SC73001.FR

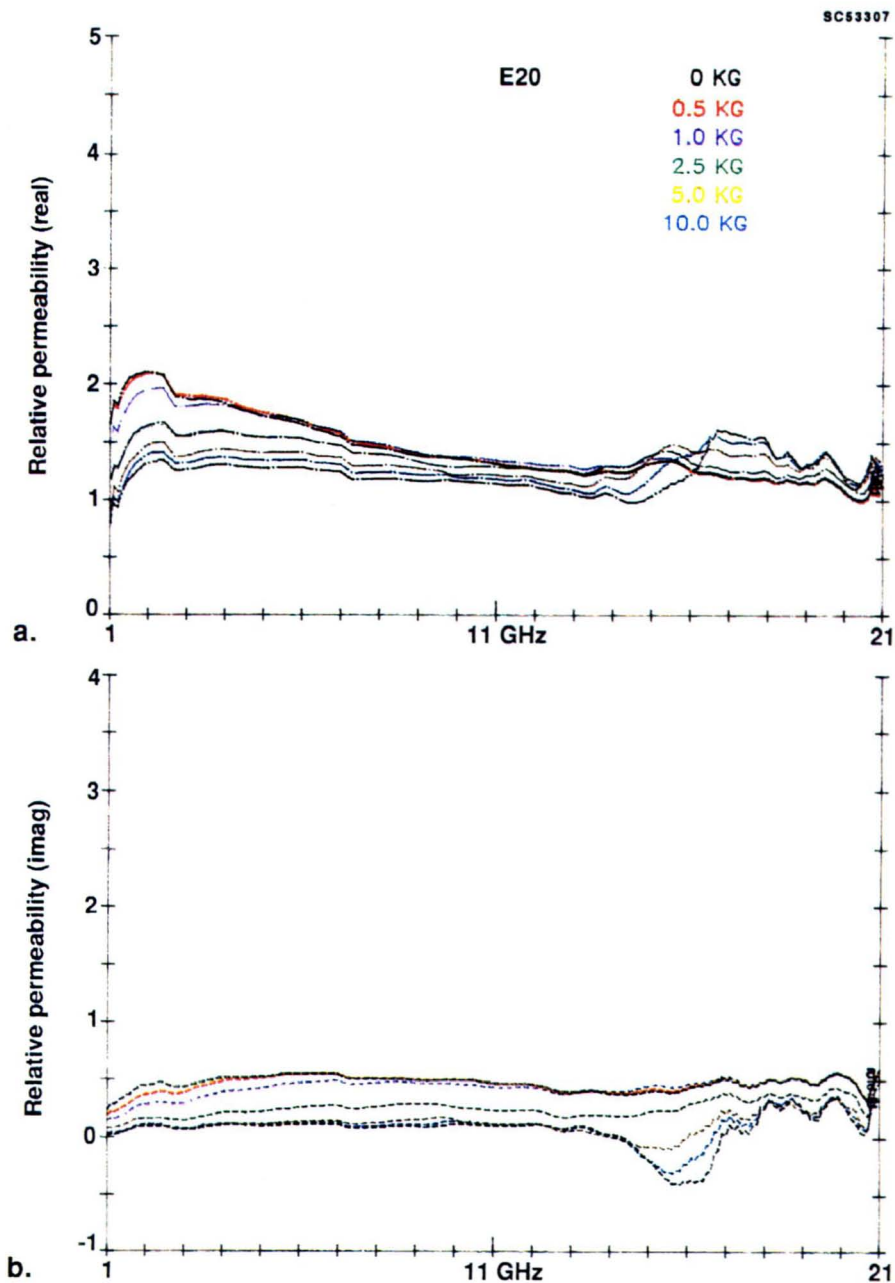


Fig. 14 Plots of the real and imaginary parts of permeability, respectively μ' and μ'' , vs frequency (GHz) for a mixture of 20% by volume E grade carbonyl iron powder in epoxy at different applied magnetic fields: (a) real part of permeability and (b) imaginary part of permeability.



A tentative conclusion is that SF and E powder could be used as a magnetic microwave absorber at magnetic fields above about 3000 Oe. However, there will be a relatively small decrease absorption in the vicinity of 1-6 GHz. Absorption between 6 and 20 GHz should be similar to or better than that in the absence of a magnetic field. More details will be given in the discussion section.

3.3.2 Cavity Perturbation Measurements

The variation of results was surprising since CIP materials should be similar. As a result cavity perturbation measurements were carried out as described above, with the principal objectives of obtaining greater precision than in transmission line measurements, but at the cost of the frequency dependence of the material. The secondary objectives of this effort were to determine the effects of the type of particle, particle size, and concentration at low concentrations.

As will be described below, if the thickness of absorbing material is not critical, then low concentrations can be used. If the concentration is low, then the demagnetization factor should approach that of individual particles.

Figures 15-18 show cavity perturbation data for four different concentrations of 60730-01, which is the as-received carbonyl iron powder before size separation (Table 2). Other than the fact that the range of frequency shift and $1/Q$ increases as the concentration increases, the samples each exhibit similar magnetic field dependencies. Because of the greater sensitivity of the perturbation measurement, the changes of the permeability with field are more evident than in the transmission line measurement, but the trend is qualitatively the same if the results at 9.5 GHz are compared. The cavity perturbation measurement shows that μ' initially increases as the field increases, but reaches a peak at 6 GHz. μ'' also increases as the field is increased, but reaches a peak at about 3 kOe. Because the ratio of μ'' to μ' is nearly constant, the absorption properties of the material will remain fairly constant up to 3 kOe. Furthermore, the relatively large μ'' makes this material acceptable. The absorption performance between 3 and about 4.5 kOe should be slightly smaller than at the lower fields, but still reasonably good. Above 4.5 kOe, the performance should deteriorate rapidly. The shapes and positions of these curves are more complex than would be expected for ferromagnetic resonance due



SC73001.FR

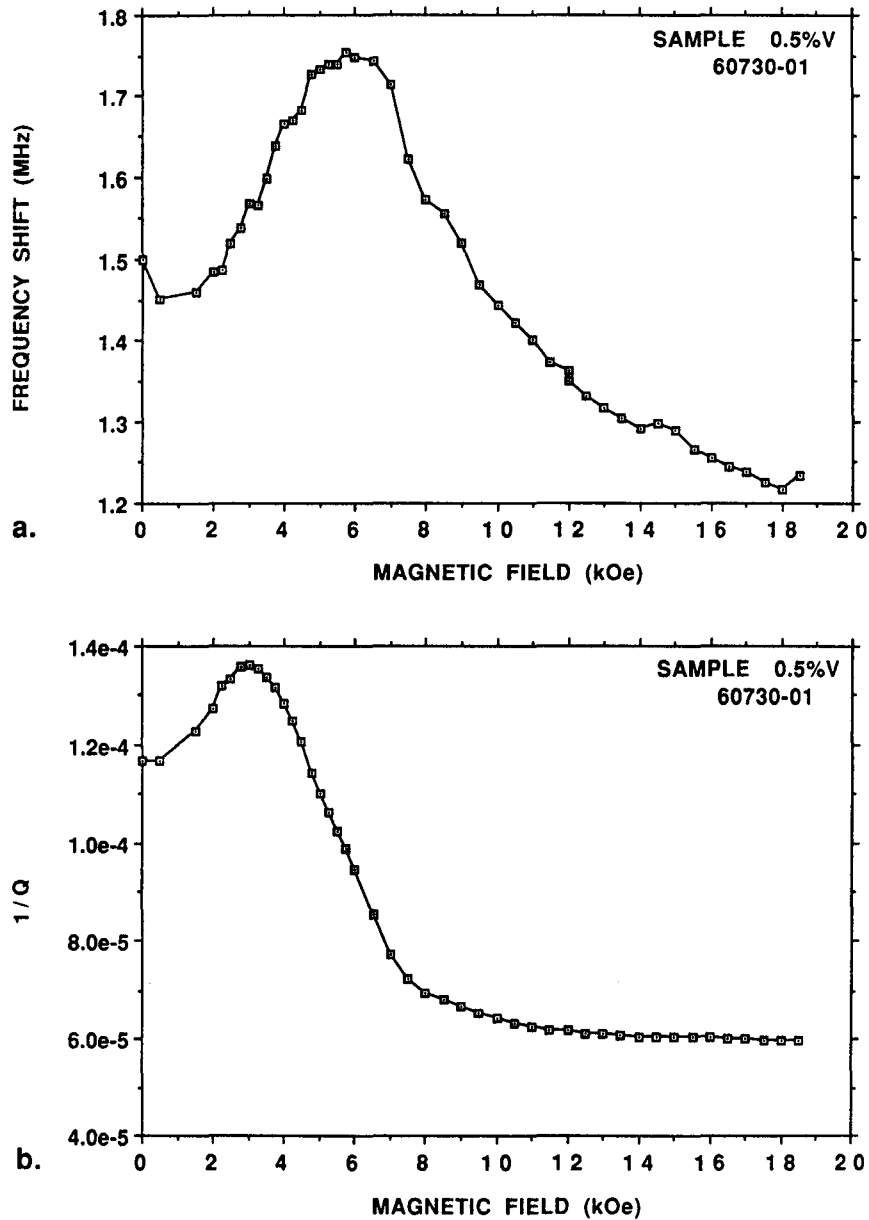


Fig. 15 Results of cavity perturbation measurements at 9.5 GHz on a 0.5% by volume sample of carbonyl iron powder 60730-01 in epoxy: (a) frequency shift vs applied magnetic field; and (b) reciprocal of the sample Q-factor vs applied field.

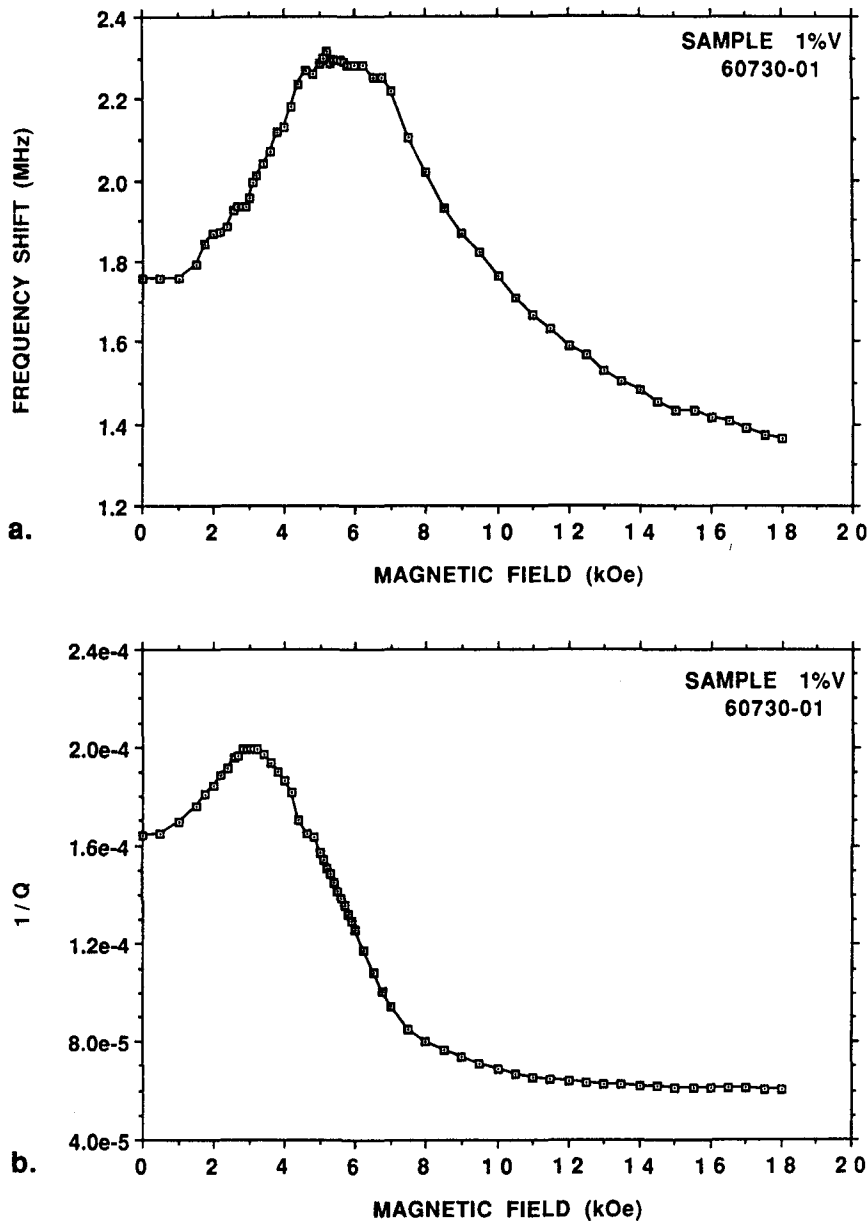


Fig. 16 Results of cavity perturbation measurements at 9.5 GHz on a 1.0% by volume sample of carbonyl iron powder 60730-01 in epoxy: (a) frequency shift vs applied magnetic field; and (b) reciprocal of the sample Q-factor vs applied field.



SC73001.FR

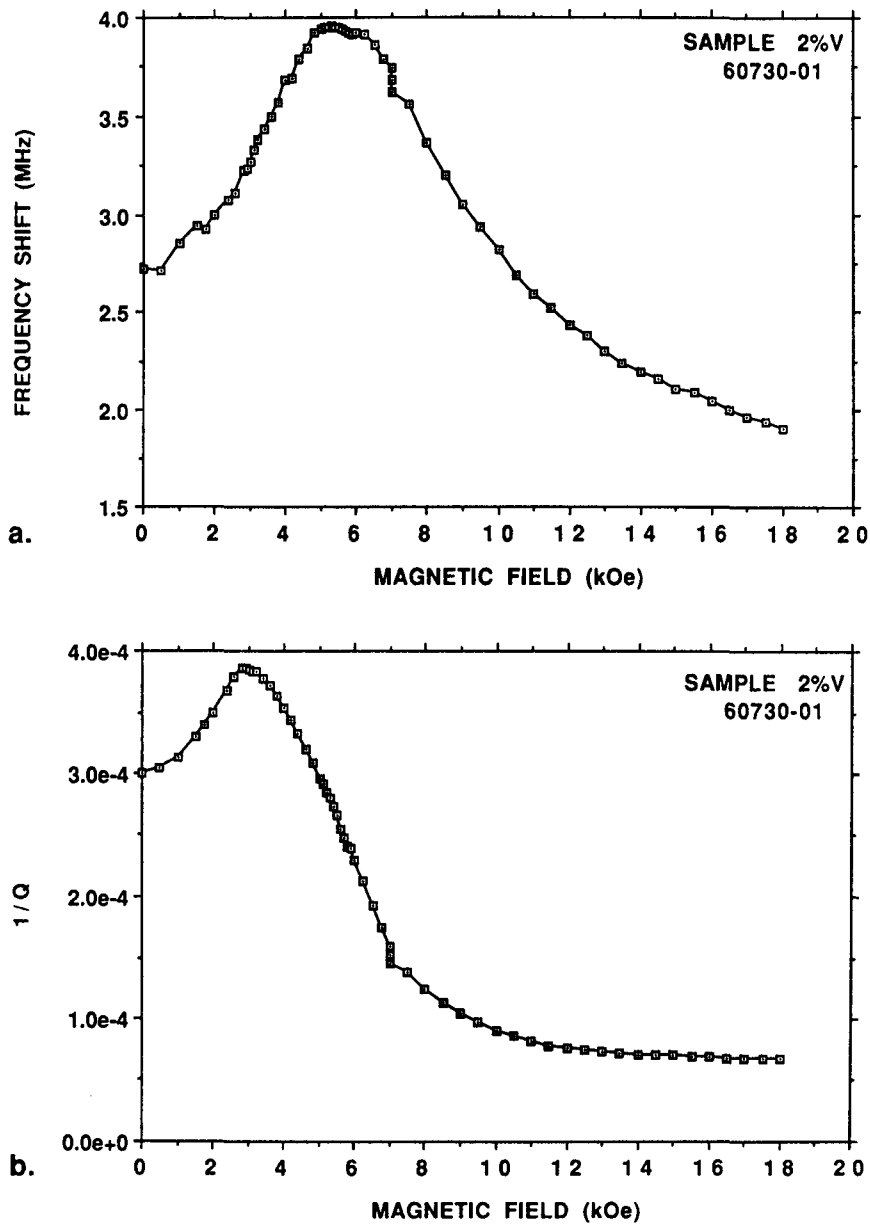


Fig. 17 Results of cavity perturbation measurements at 9.5 GHz on a 2.0% by volume sample of carbonyl iron powder 60730-01 in epoxy: (a) frequency shift vs applied magnetic field; and (b) reciprocal of the sample Q-factor vs applied field.

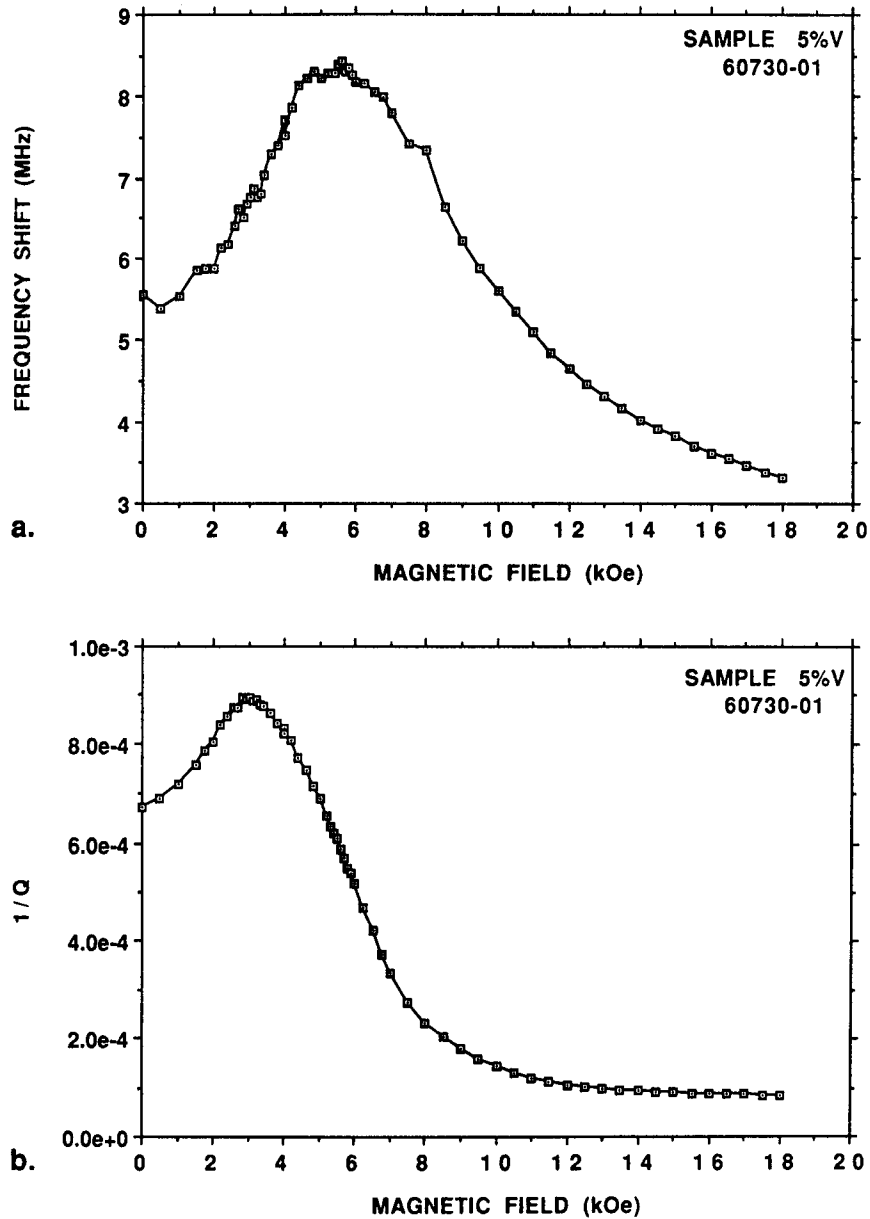


Fig. 18 Results of cavity perturbation measurements at 9.5 GHz on a 5.0% by volume sample of carbonyl iron powder 60730-01 in epoxy: (a) frequency shift vs applied magnetic field; and (b) reciprocal of the sample Q-factor vs applied field.



to spherical particles.⁷ Neither the frequency shift nor the $1/Q$ for the sample approach the limiting value of the cavity and blank sample due to residual eddy current effects. Even for a diamagnetic sample, there is still some permeability due to eddy current losses.

Sample 60730-01 was fractionated into different size fractions under Rockwell IR&D. The availability of these size fractions permitted us determine differences in the behavior due to size, with minimum variation of other parameters. The largest mean particle size of any fraction was $1.848\ \mu\text{m}$. Size fraction 60730-05 exhibited a mean diameter of $1.168\ \mu\text{m}$. Cavity perturbation data for this sample are shown in Figs. 19 and 20. Once again, concentration between 0.5 and 5% by volume exhibits relatively little effect on the shape of the field dependence of the frequency shift or Q -factor. The major distinctions of these samples relative to the -01 sample are that the frequency shift does not increase as much and $1/Q$ decreases significantly as the magnetic field strength is increased. This suggests that the material is more easily magnetized by the application of an external field. As a result, such material would not be as effective a microwave absorber.

Cavity perturbation data for sample 60730-08 are shown in Figs. 21 and 22. Here the particle size is slightly larger than for sample -01, but smaller than that of -01. The magnetic field dependence of both the frequency shift and $1/Q$ are intermediate between samples 60730-01 and -05. Most significant is that $1/Q$ (or μ'') changes only slightly as the magnetic field is increased. Concentration has a small but noticeable effect of the shapes of these curves.

Cavity perturbation data for sample 60730-13 are shown in Figs. 23-26. Here the particle size is about the same as for sample -05, and the magnetic field dependence is similar.

Sample GS6 is a carbonyl iron powder annealed in hydrogen. As a result the "onionskin" layered structure characteristic of most of the CIPs is removed, and the material is more representative of pure iron. Cavity perturbation data for this sample at four concentrations are shown in Figs. 27-30. As in the case of other samples, the concentration exhibits little effect on the magnetic field dependence of the frequency shift or $1/Q$. In all cases, the frequency shift increases with magnetic field and reaches a



SC73001.FR

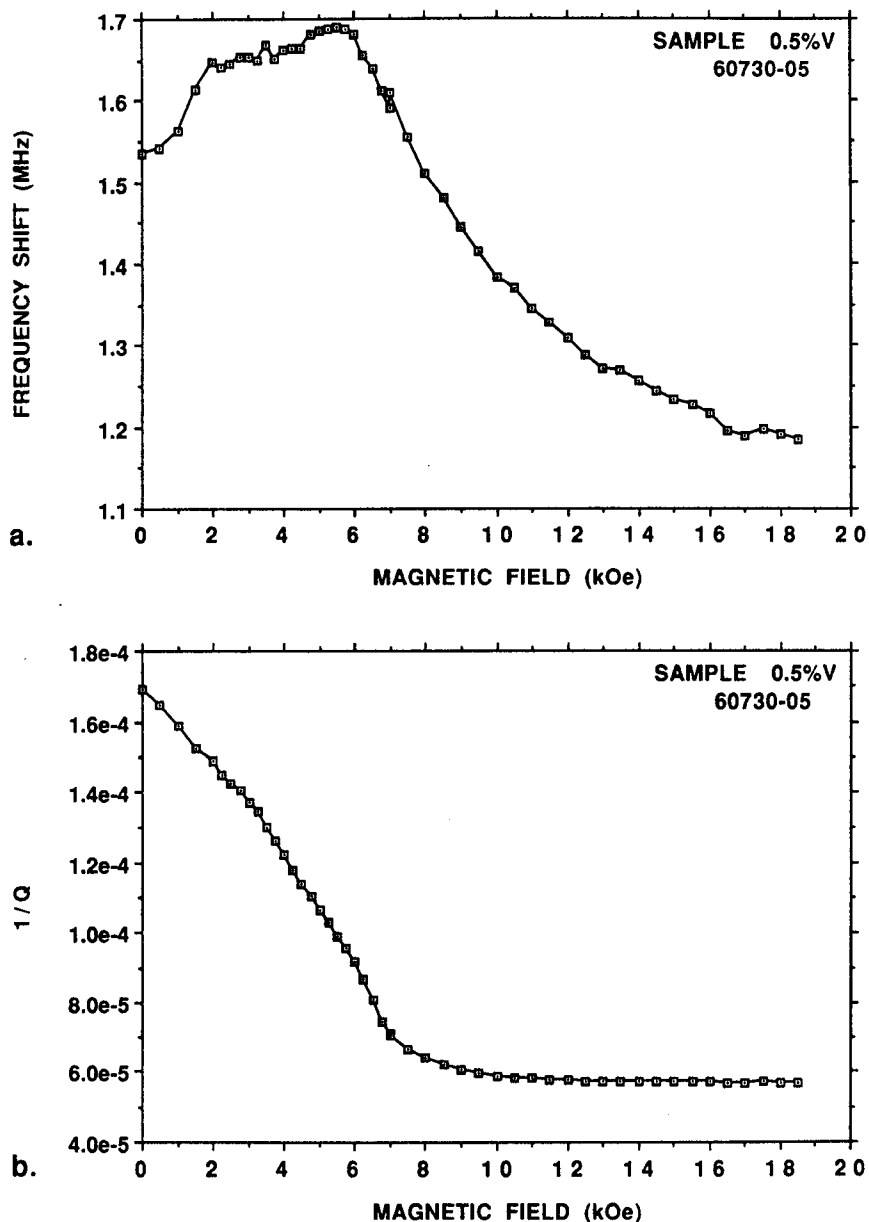


Fig. 19 Results of cavity perturbation measurements at 9.5 GHz on a 0.5% by volume sample of carbonyl iron powder 60730-05 in epoxy: (a) frequency shift vs applied magnetic field; and (b) reciprocal of the sample Q-factor vs applied field.



SC73001.FR

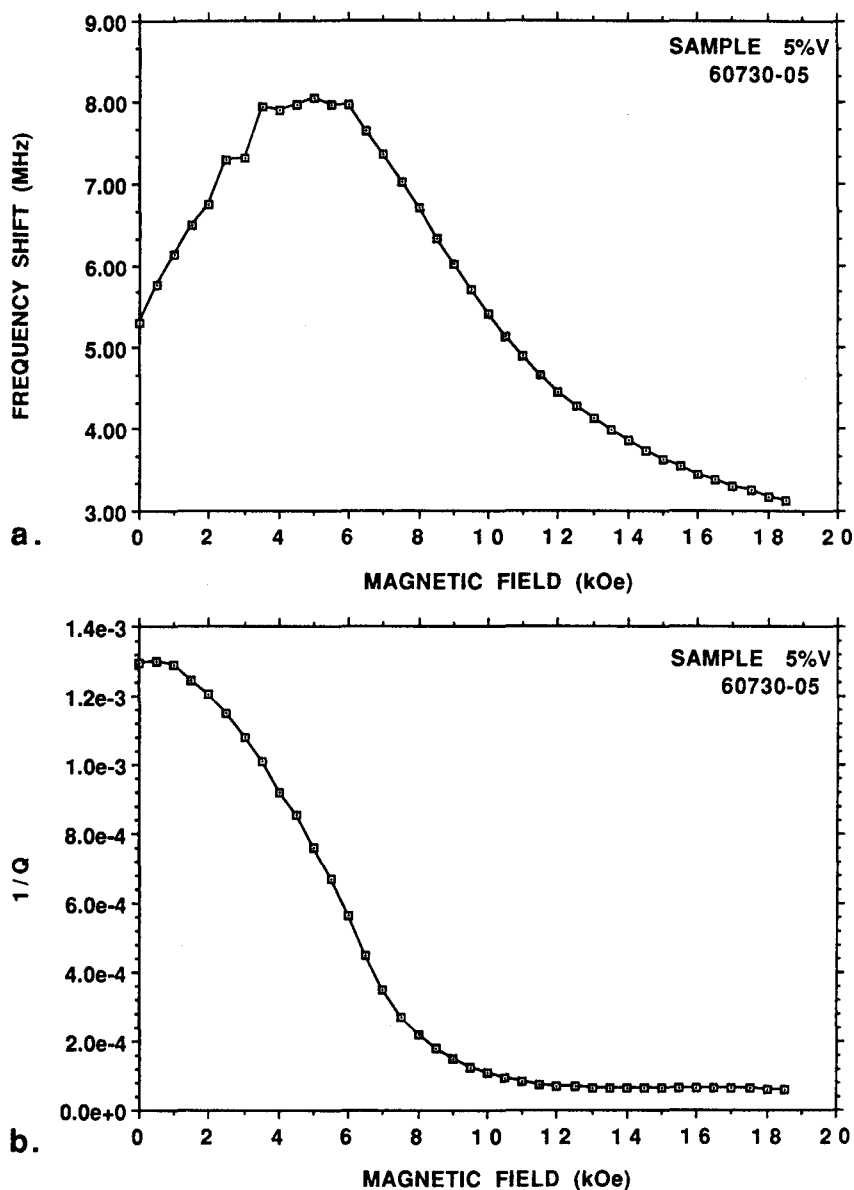


Fig. 20 Results of cavity perturbation measurements at 9.5 GHz on a 5.0% by volume sample of carbonyl iron powder 60730-05 in epoxy: (a) frequency shift vs applied magnetic field; and (b) reciprocal of the sample Q-factor vs applied field.



SC73001.FR

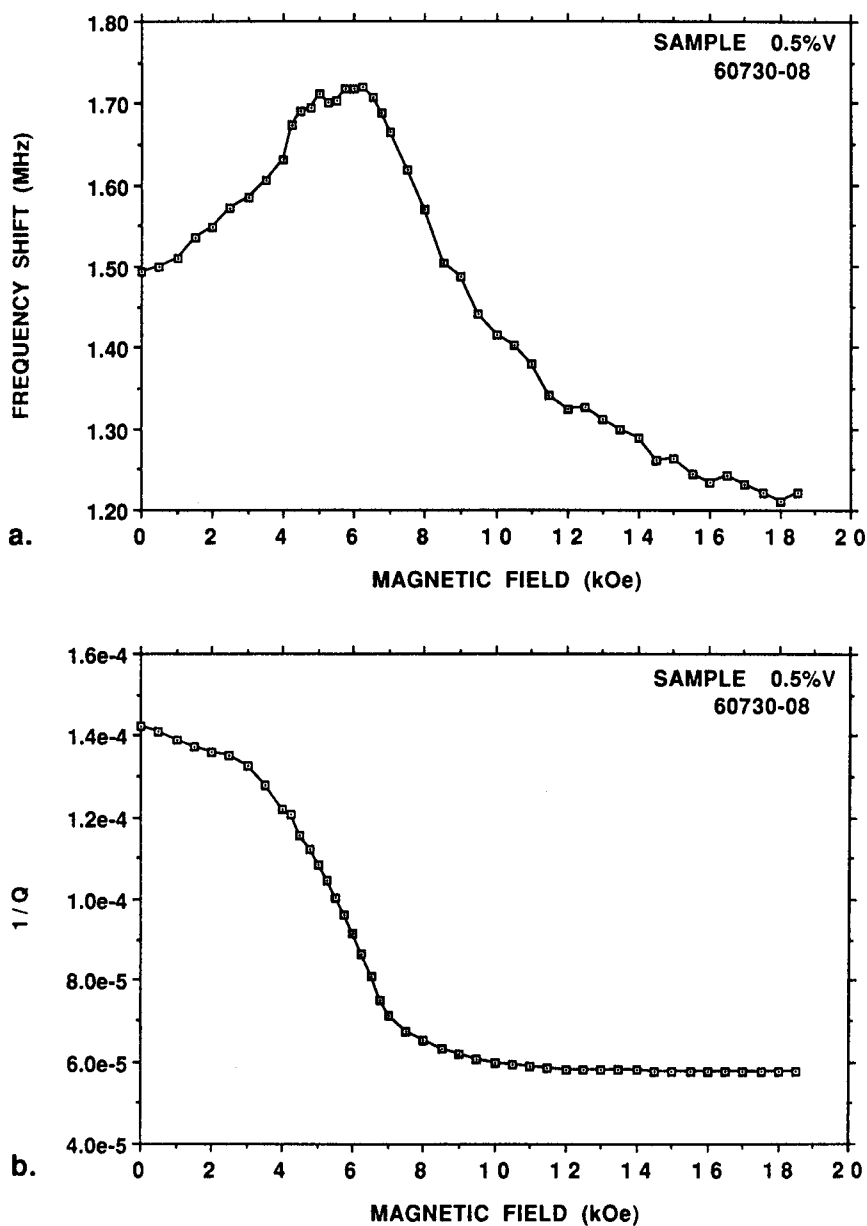


Fig. 21 Results of cavity perturbation measurements at 9.5 GHz on a 0.5% by volume sample of carbonyl iron powder 60730-08 in epoxy: (a) frequency shift vs applied magnetic field; and (b) reciprocal of the sample Q-factor vs applied field.

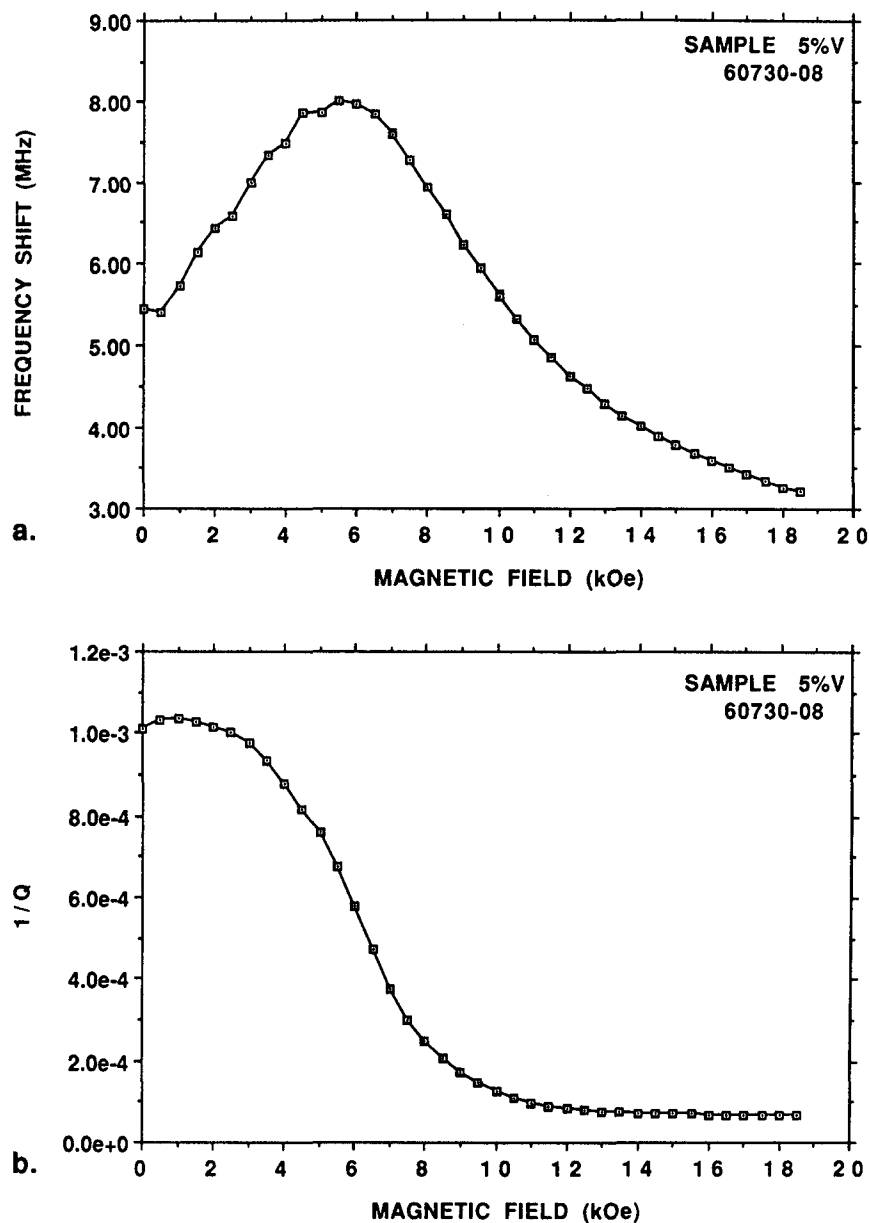


Fig. 22 Results of cavity perturbation measurements at 9.5 GHz on a 5.0% by volume sample of carbonyl iron powder 60730-08 in epoxy: (a) frequency shift vs applied magnetic field; and (b) reciprocal of the sample Q-factor vs applied field.

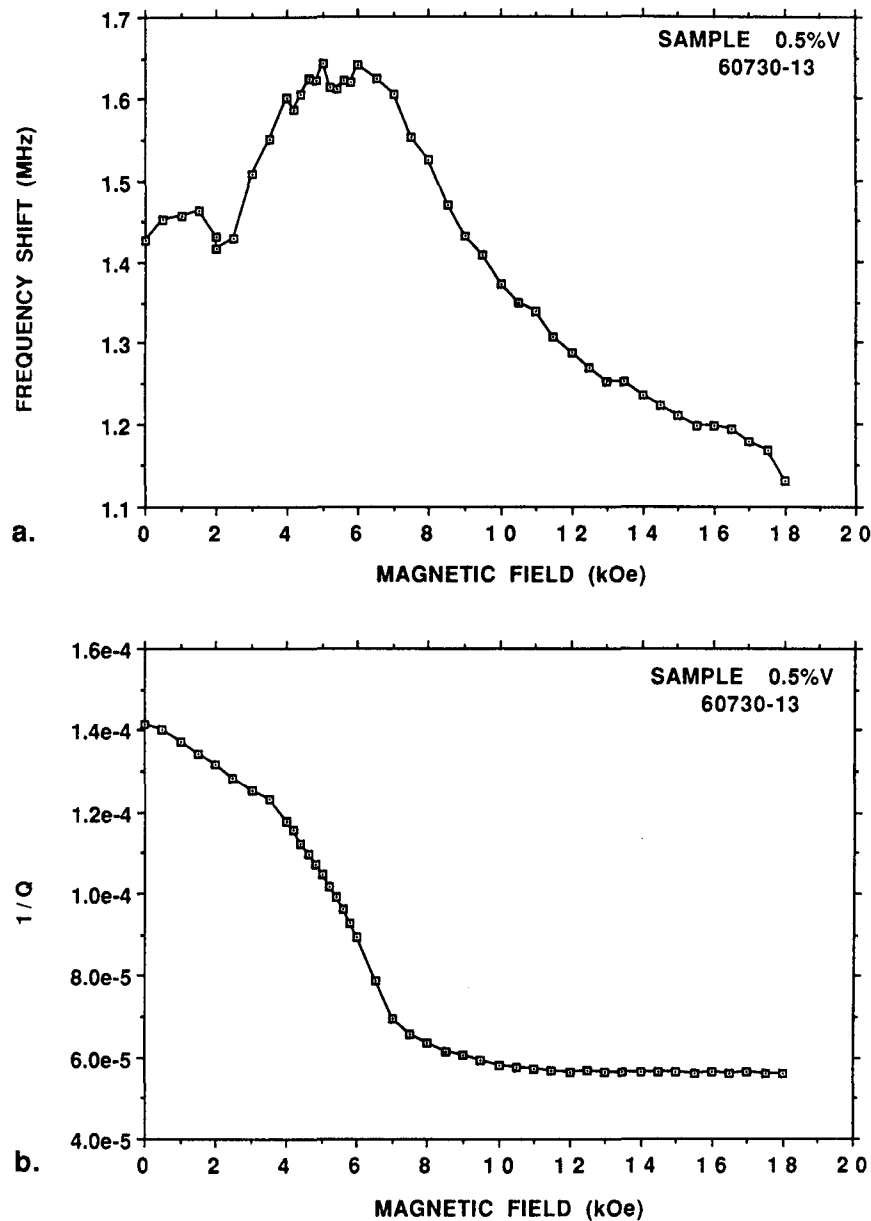


Fig. 23 Results of cavity perturbation measurements at 9.5 GHz on a 0.5% by volume sample of carbonyl iron powder 60730-13 in epoxy: (a) frequency shift vs applied magnetic field; and (b) reciprocal of the sample Q-factor vs applied field.



SC73001.FR

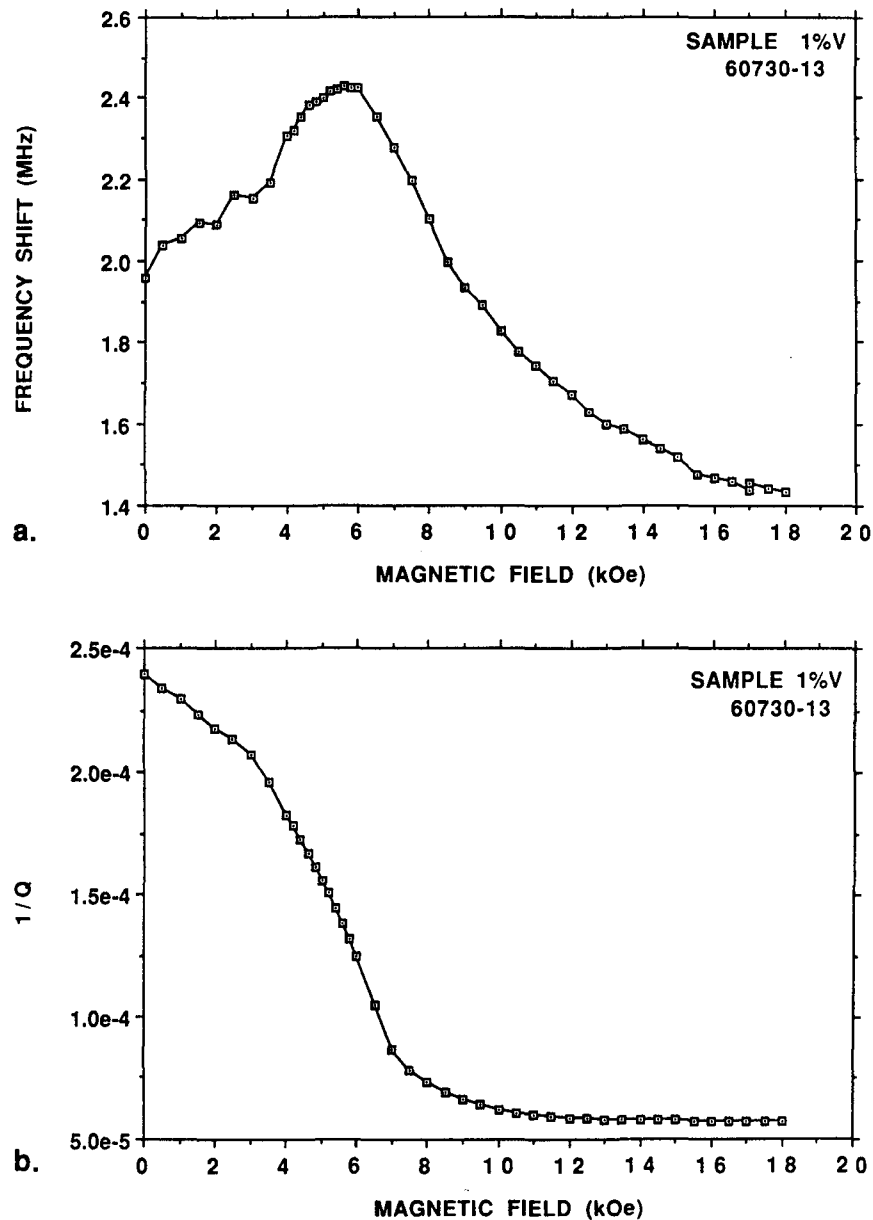


Fig. 24 Results of cavity perturbation measurements at 9.5 GHz on a 1.0% by volume sample of carbonyl iron powder 60730-13 in epoxy: (a) frequency shift vs applied magnetic field; and (b) reciprocal of the sample Q-factor vs applied field.

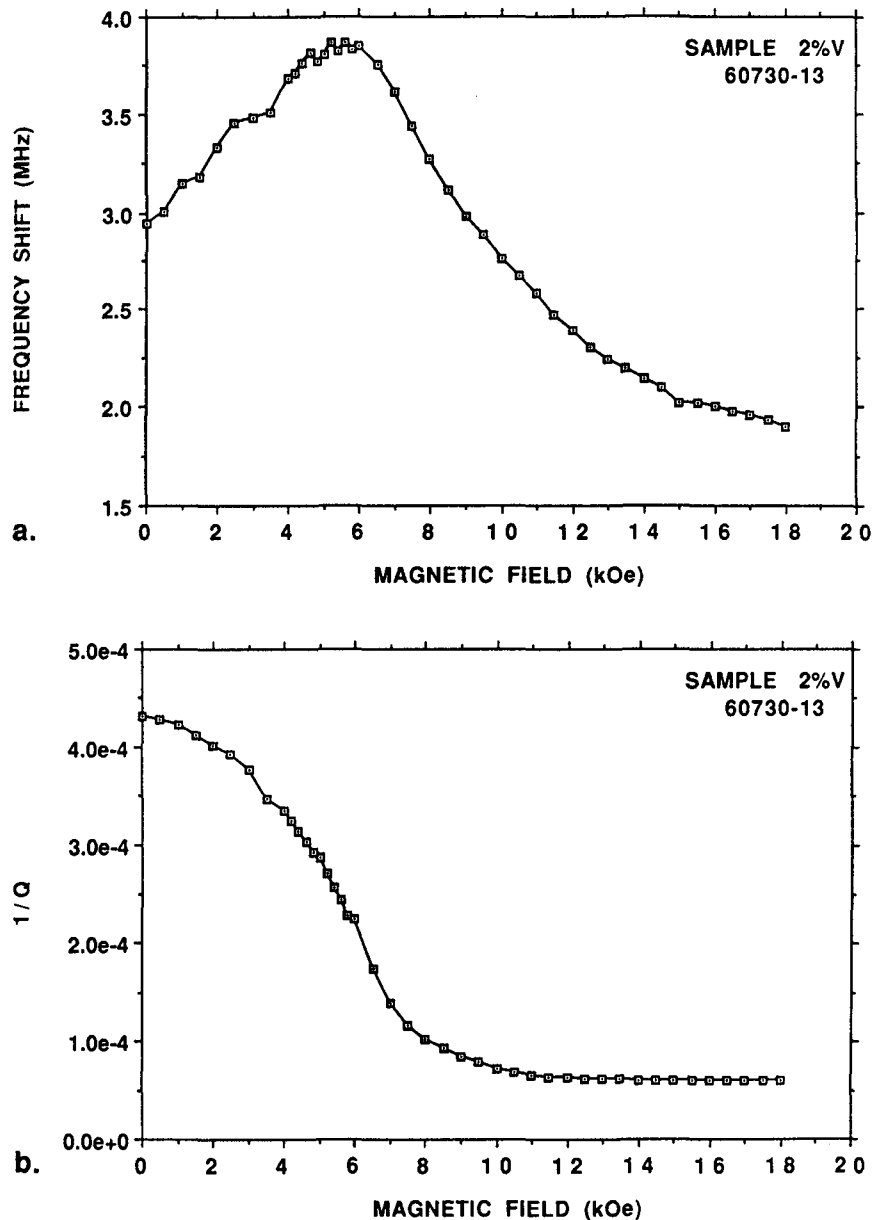


Fig. 25 Results of cavity perturbation measurements at 9.5 GHz on a 2.0% by volume sample of carbonyl iron powder 60730-13 in epoxy: (a) frequency shift vs applied magnetic field; and (b) reciprocal of the sample Q-factor vs applied field.



SC73001.FR

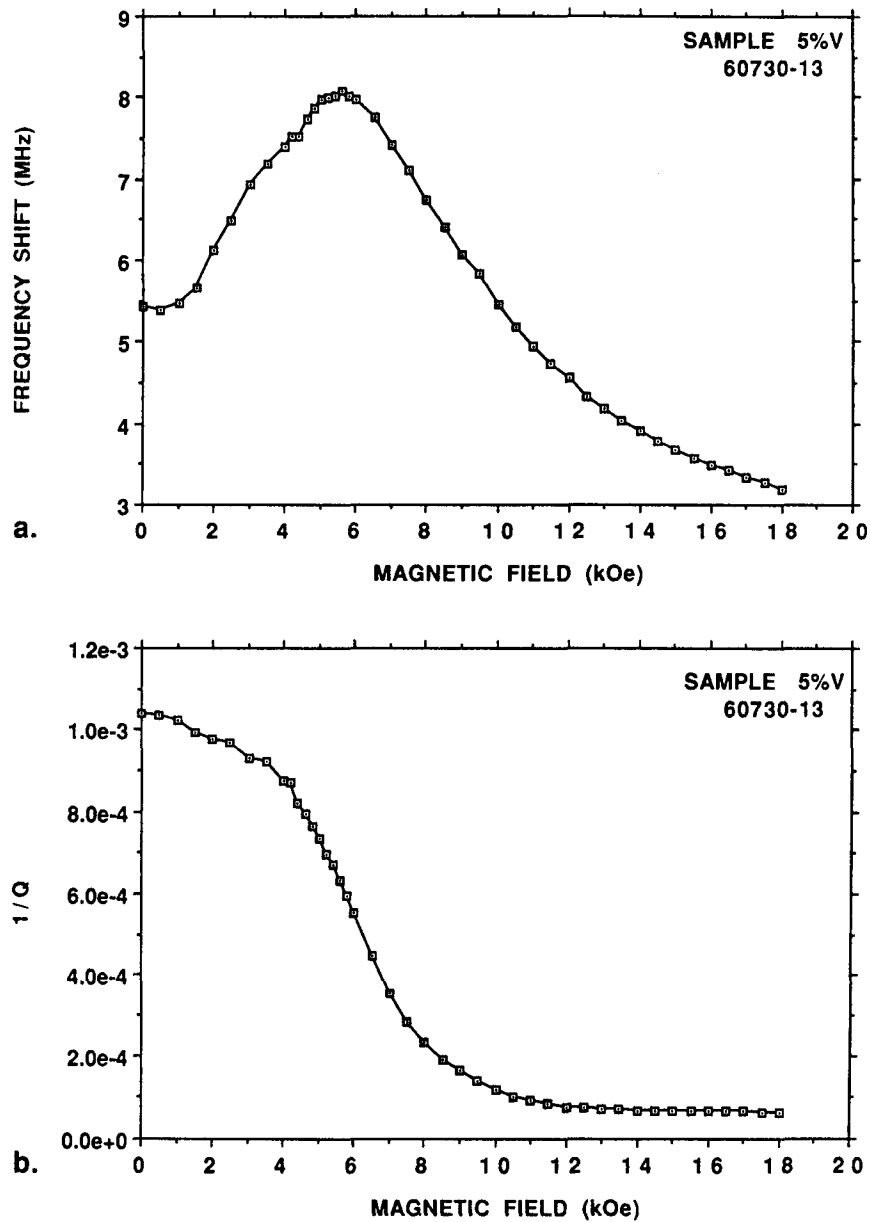


Fig. 26 Results of cavity perturbation measurements at 9.5 GHz on a 5.0% by volume sample of carbonyl iron powder 60730-13 in epoxy: (a) frequency shift vs applied magnetic field; and (b) reciprocal of the sample Q-factor vs applied field.



SC73001.FR

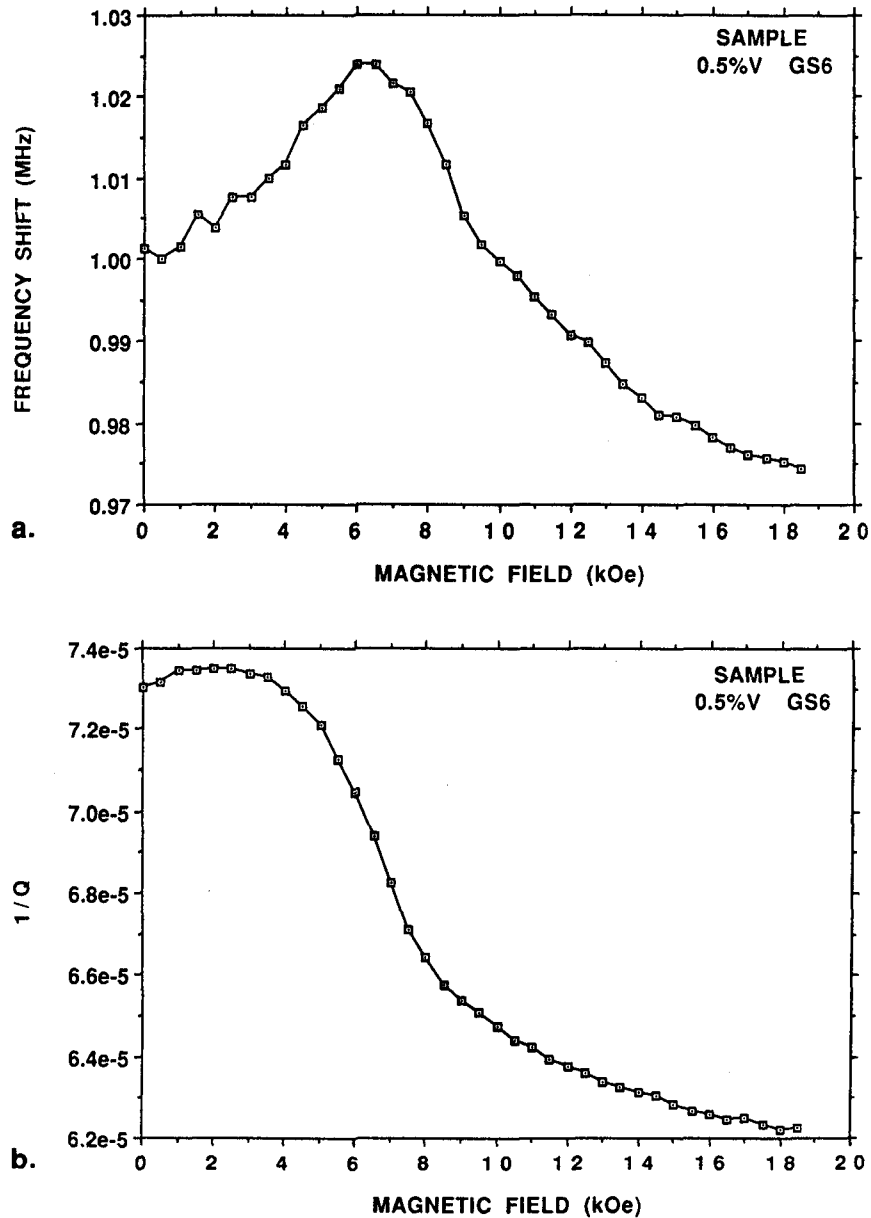


Fig. 27 Results of cavity perturbation measurements at 9.5 GHz on a 0.5% by volume sample of GS6 carbonyl iron powder in epoxy: (a) frequency shift vs applied magnetic field; and (b) reciprocal of the sample Q-factor vs applied field.



SC73001.FR

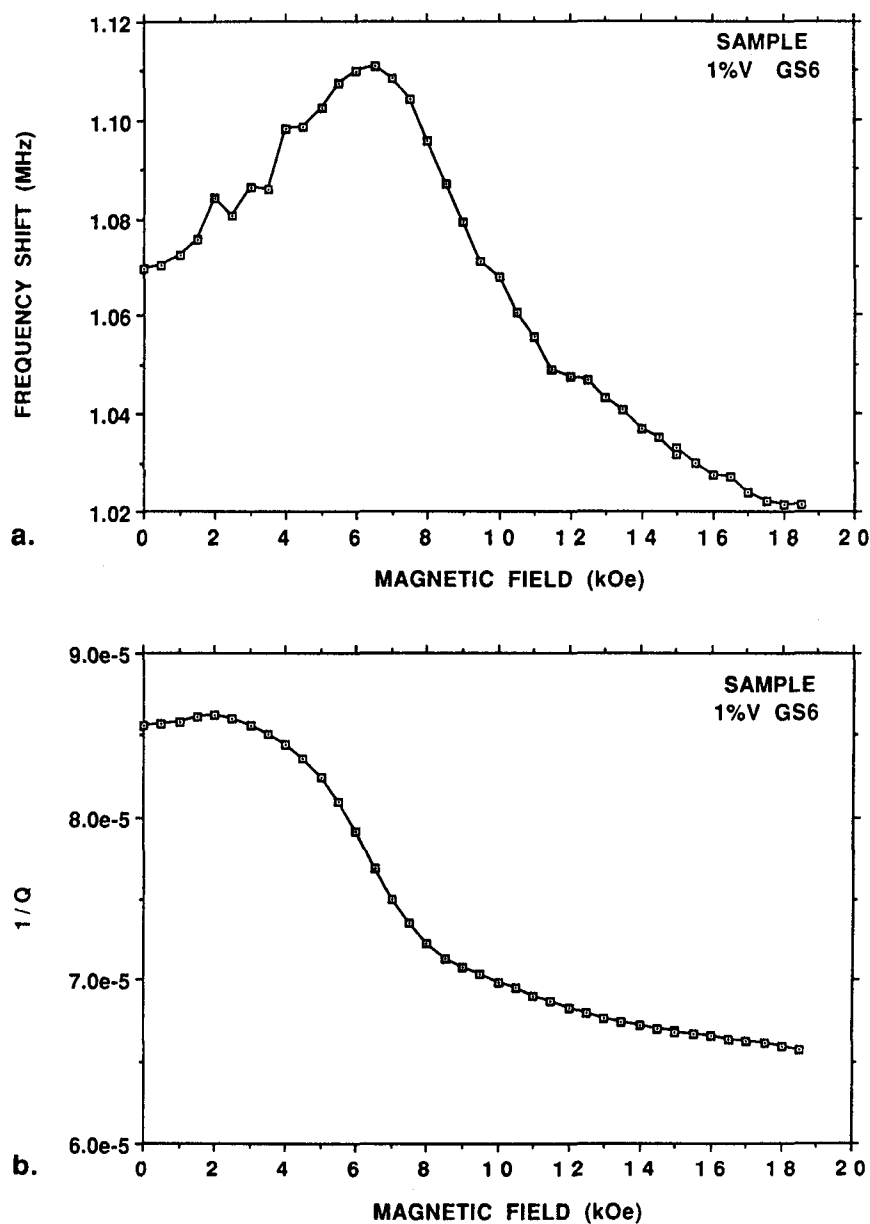


Fig. 28 Results of cavity perturbation measurements at 9.5 GHz on a 1.0% by volume sample of GS6 carbonyl iron powder in epoxy: (a) frequency shift vs applied magnetic field; and (b) reciprocal of the sample Q-factor vs applied field.



SC73001.FR

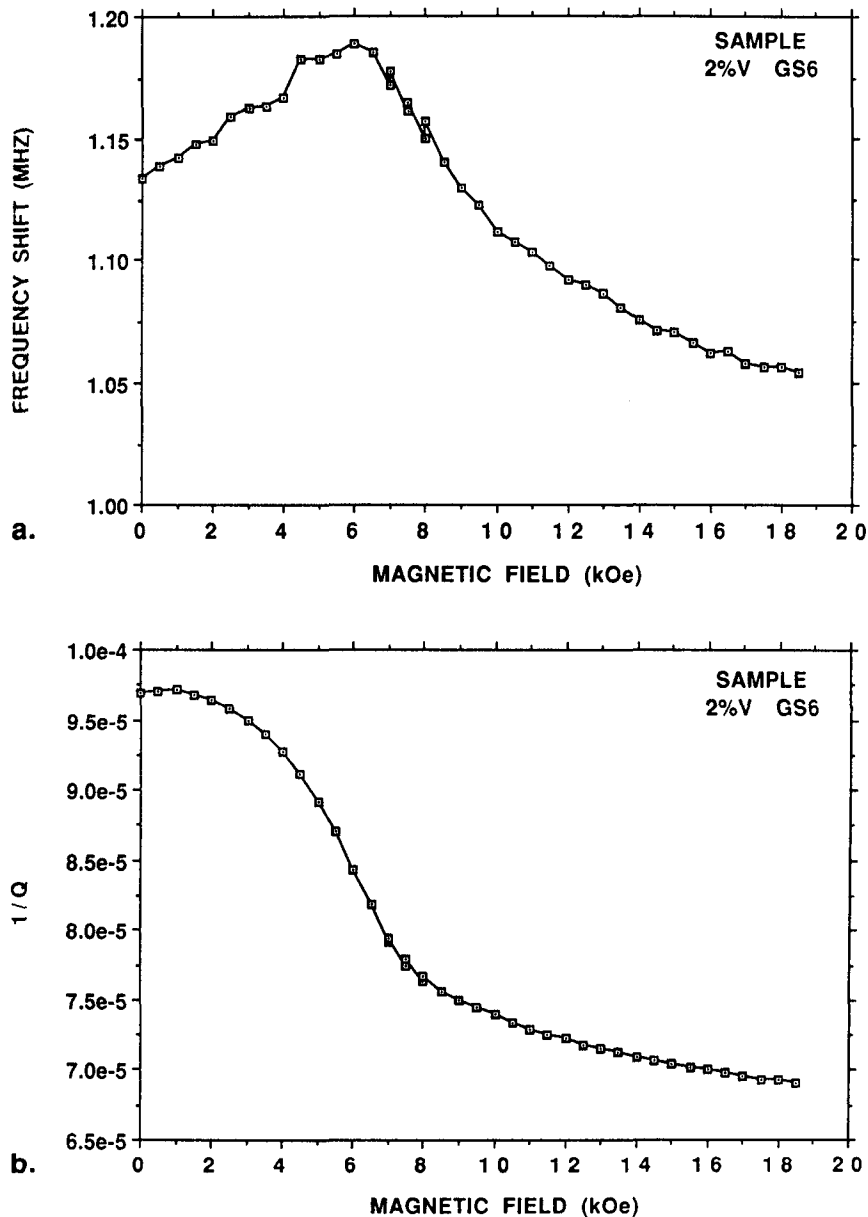


Fig. 29 Results of cavity perturbation measurements at 9.5 GHz on a 2.0% by volume sample of GS6 carbonyl iron powder in epoxy: (a) frequency shift vs applied magnetic field; and (b) reciprocal of the sample Q-factor vs applied field.



SC73001.FR

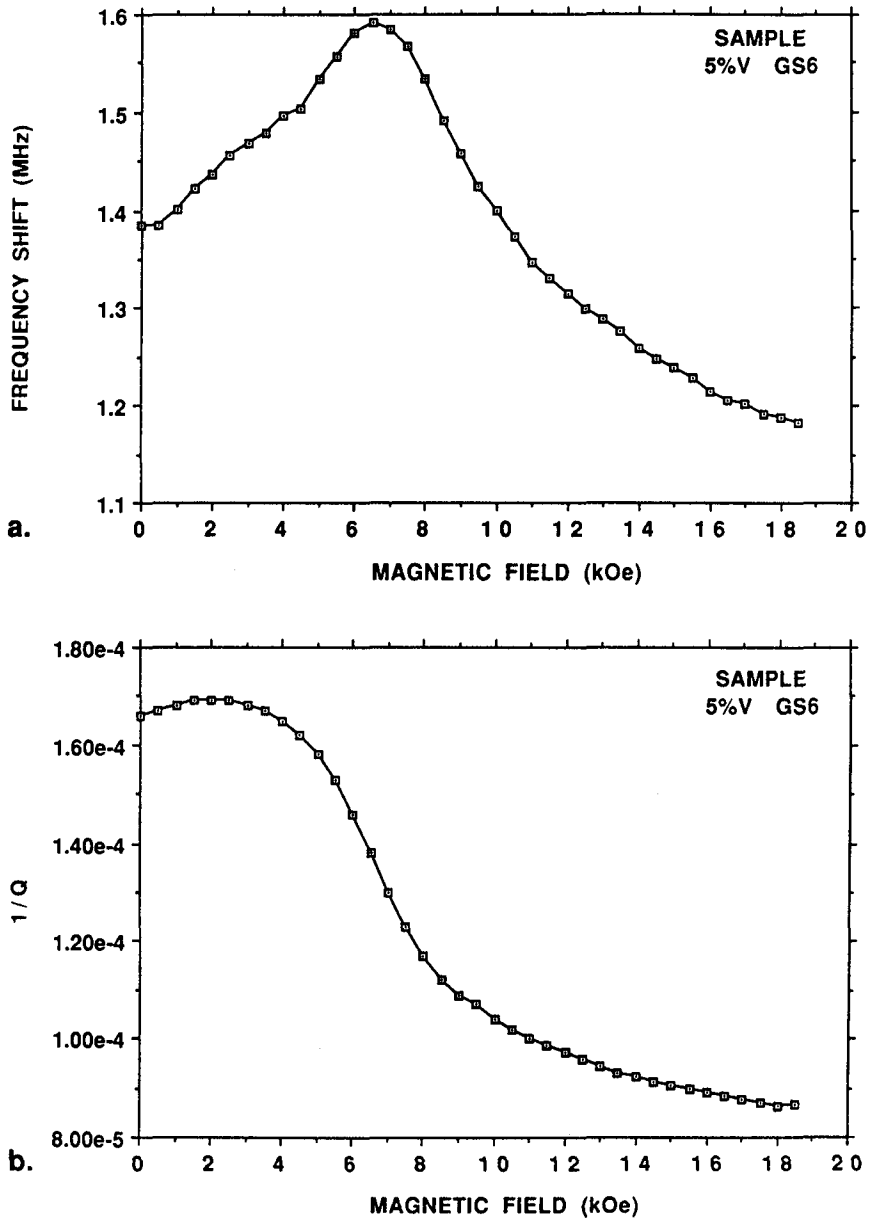


Fig. 30 Results of cavity perturbation measurements at 9.5 GHz on a 5.0% by volume sample of GS6 carbonyl iron powder in epoxy: (a) frequency shift vs applied magnetic field; and (b) reciprocal of the sample Q-factor vs applied field.



maximum at about 6 kOe. Only a small increase in $1/Q$ is observed as the magnetic field is increased. However, this sample is substantially different from the other materials in that the ranges of both the frequency shift and $1/Q$ are smaller than for the previous powders. As a result, both μ' and μ'' are smaller than for the 60730 series powders. This means that GS6 is not nearly as good an absorber.

Cavity perturbation data for a sample of 2% SF Special are shown in Fig. 31. The mean particle size is close to those of samples 60730-05 and -13. However, if the sample diameter determined from the mean volume is considered, this powder is significantly finer than the other two powders. This occurs because the mean volume is calculated by integrating d^3 , so that larger particle sizes are weighted more than the smaller ones. As in previous samples the frequency shift increases and reaches a peak at about 5.5 kOe. Based on the previous results however, $1/Q$ or μ'' would be expected to decrease with applied field. Nevertheless, there is a small increase as the field increases, and the peak value occurs at 2.5 Koe. For this powder, the magnitude of μ'' is not as large as for other powders.

Similar measurements are shown for 2% EW powder in Fig. 32. Here $1/Q$ shows similar behavior to sample 60730-01, but the frequency shift shows a sharp peak rather than a rounded one. A distinction between the powders produced by GAF and BASF is that the BASF powders are produced at a higher temperature than those at GAF. Although the higher temperature may cause a slightly different grain structure, the particles tend to form some nodules on the side decreasing the sphericity from those produced at lower temperatures. Nevertheless, this appears to be reasonably good material.

Cavity perturbation data for a sample of 2% W powder are shown in Fig. 33. These data appear similar in magnitude and shape to the GS6 powder. Since nitrided powder is first reduced in hydrogen before reaction with ammonia, it probably exhibits similar size and structure to GS6.

Cavity perturbation data for a sample of 2% KX carbonyl iron powder are shown in Fig. 34. This powder is coarser than most, but is also far less spherical than all of the other powders tested. The frequency shift and $1/Q$ are smaller than the other samples of 2% by volume, resulting in smaller values for μ' and μ'' . The frequency shift is similar to those determined for other powders, but it is flatter at the peak. Only a small increase in $1/Q$ is observed for this material.

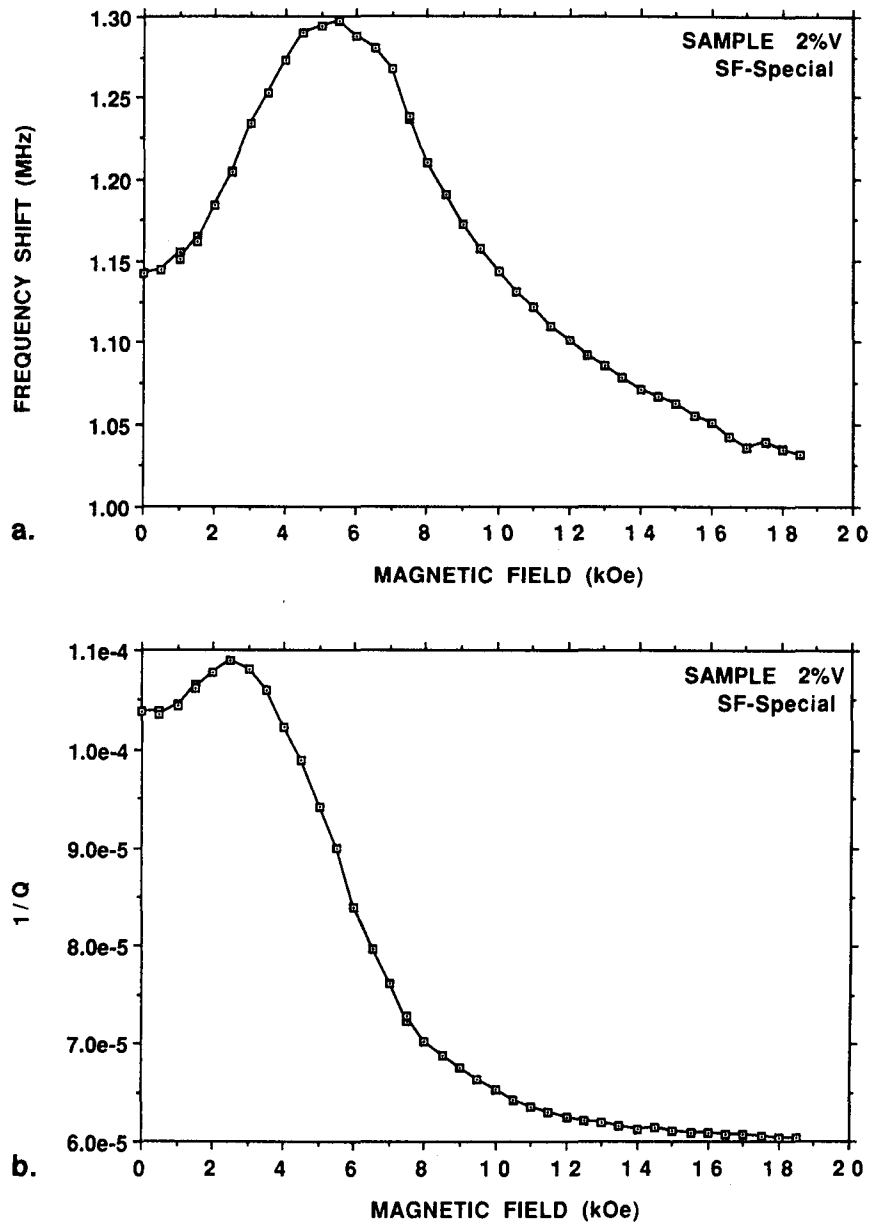


Fig. 31 Results of cavity perturbation measurements at 9.5 GHz on a 2.0% by volume sample of SF Special carbonyl iron powder in epoxy: (a) frequency shift vs applied magnetic field; and (b) reciprocal of the sample Q-factor vs applied field.



SC73001.FR

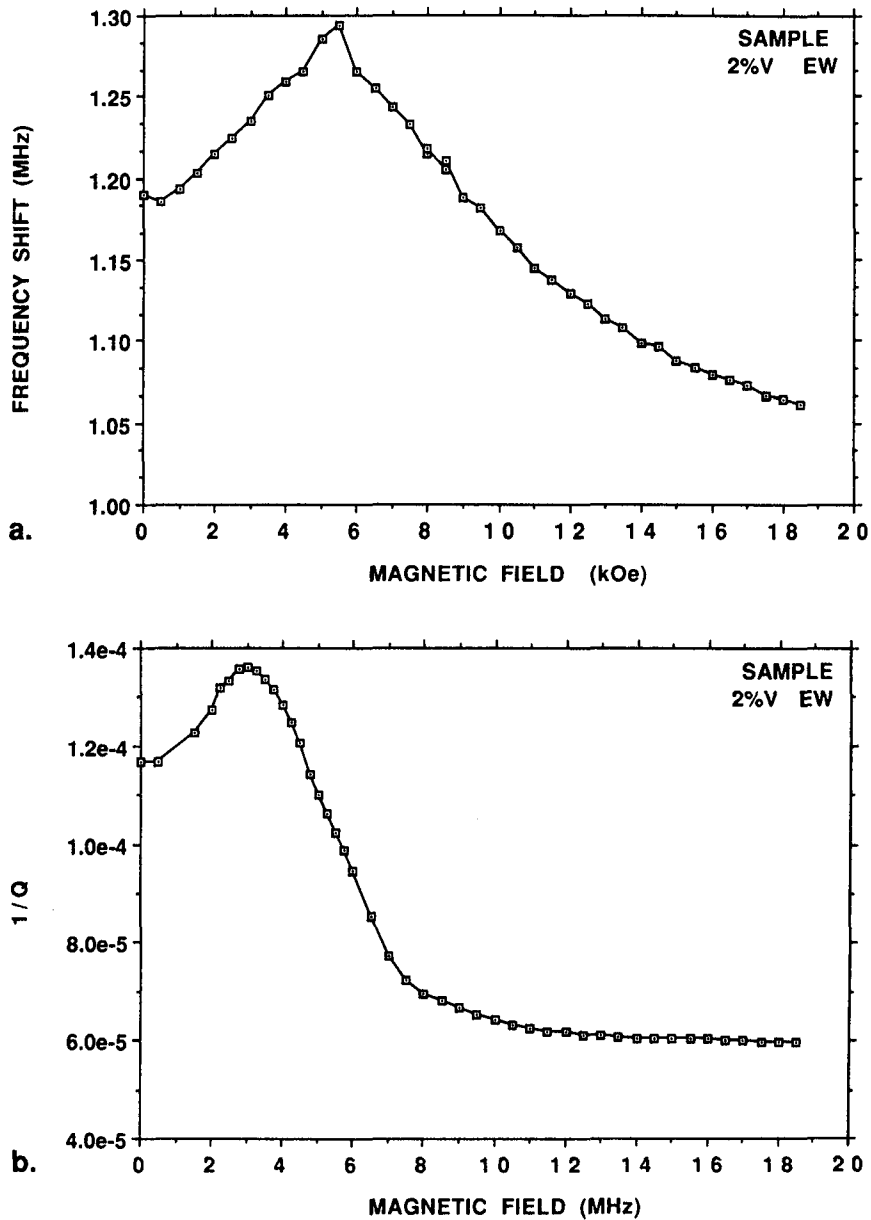


Fig. 32 Results of cavity perturbation measurements at 9.5 GHz on a 2.0% by volume sample of EW carbonyl iron powder in epoxy: (a) frequency shift vs applied magnetic field; and (b) reciprocal of the sample Q-factor vs applied field.



SC73001.FR

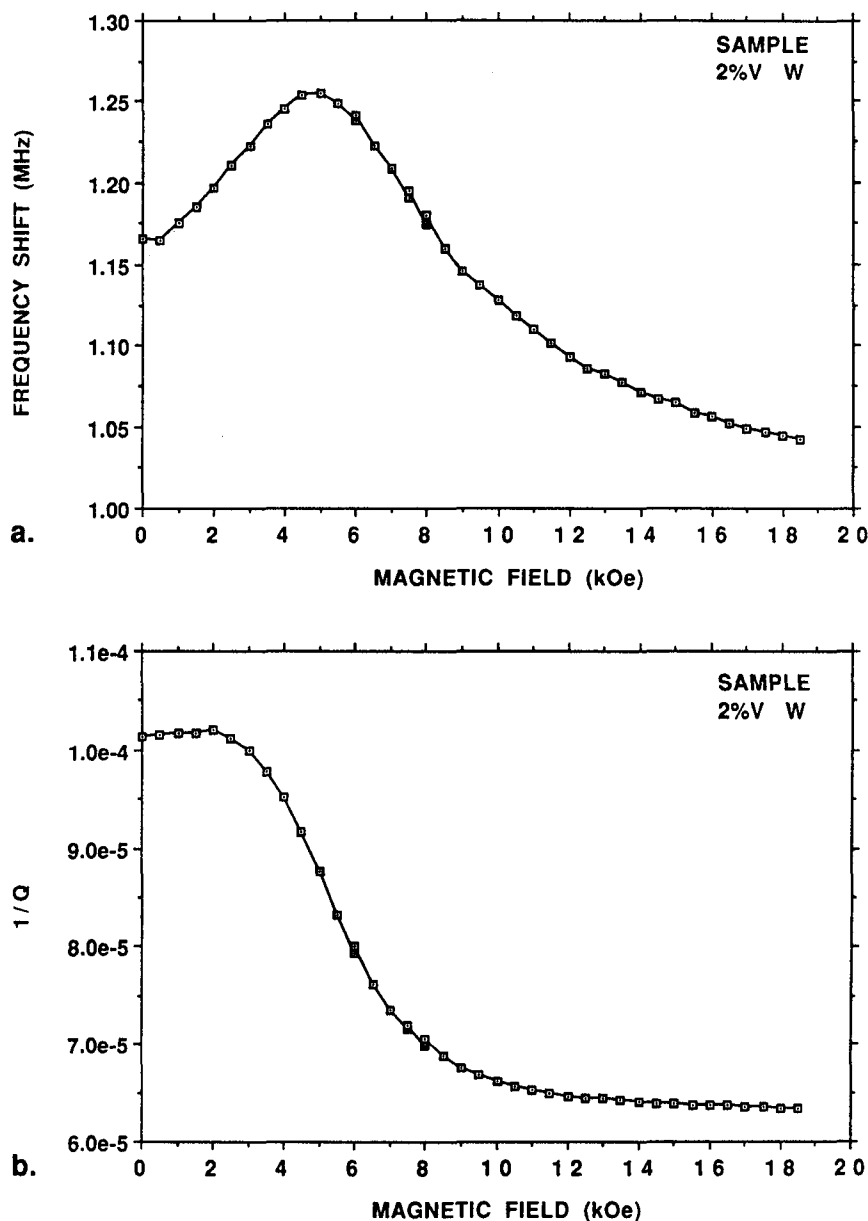


Fig. 33 Results of cavity perturbation measurements at 9.5 GHz on a 2.0% by volume sample of carbonyl iron powder W in epoxy: (a) frequency shift vs applied magnetic field; and (b) reciprocal of the sample Q-factor vs applied field.



SC73001.FR

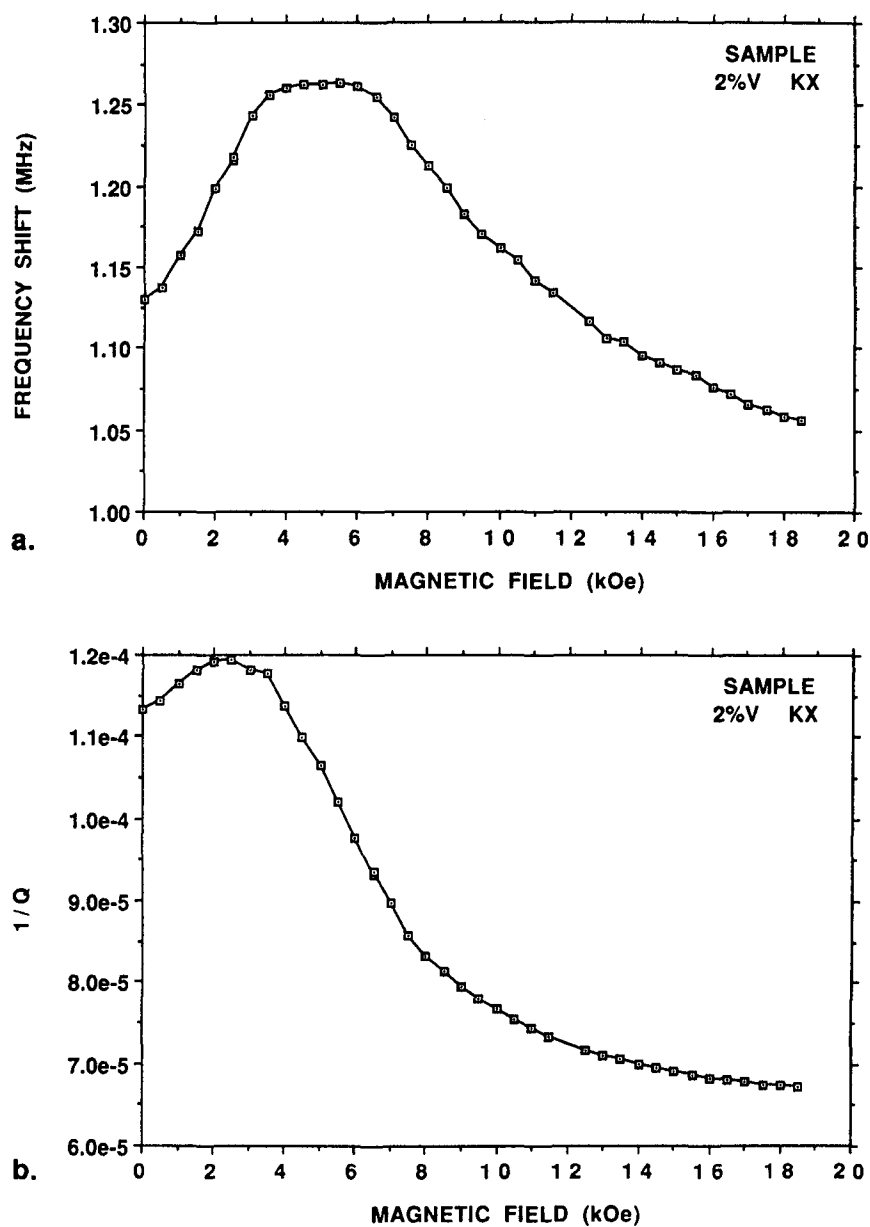


Fig. 34 Results of cavity perturbation measurements at 9.5 GHz on a 2.0% by volume sample of carbonyl iron powder KX in epoxy: (a) frequency shift vs applied magnetic field; and (b) reciprocal of the sample Q-factor vs applied field.



4.0 CONCLUSIONS AND DISCUSSION OF RESULTS

4.1 General Performance

The results of the measurements show that carbonyl iron powders can be used as microwave absorbing materials at magnetic fields greater than 3 kOe. There are not enormous differences among the powders tested. In general, as the magnetic field is increased from 0 to about 6 kOe, values of μ' decrease for frequencies up to about 3 GHz, and increase for those in the range of 6 to 13 GHz. Small changes are observed at higher frequencies. Above fields of about 3 kOe, μ' decreases over the entire frequency range studied. The behavior of μ'' is slightly different and somewhat more dependent on the specific material. From about 0 to 3 kOe, μ'' generally decreases for frequencies from 0-6 GHz. Above 6 GHz, μ'' can either increase or decrease, depending on the material. When the field is increased above 3 kOe, μ'' decreases over the entire frequency range. In addition, certain resonances were detected at fields of 5 kOe or more at frequencies above 12 GHz. Cavity perturbation measurements at 9.5 GHz showed specific cases where the dependence of μ' and μ'' on magnetic field depended strongly on materials.

In general, only the magnitude of μ' and μ'' depended on concentration. The shapes of the curves, whether μ' or μ'' vs applied magnetic field at fixed frequency or μ' or μ'' vs frequency at fixed magnetic field, for a given material, appeared to scale with concentration.

As described above, many factors contribute to the permeability of a material. In general, when a material approaches saturation, the only sources of permeability are ferromagnetic resonance and eddy currents. The maximum amplitude for ferromagnetic resonance absorption due to saturated iron spheres is given by

$$f = g \mu_B H/h \quad (18)$$

where g is the spectroscopic splitting factor (2.067 for Fe), μ_B is the Bohr magneton, and h is Planck's constant. In terms of frequency, this is 2.893 MHz/Oe. For 9.5 GHz, the resonance maximum would be 3.3 kOe. This is close to where some of the peak values of μ'' occur. However, the iron is not magnetically saturated at this field. If these samples



exhibited ferromagnetic resonance in the usual way, μ' should be close to 1 when μ'' is a maximum. Ferromagnetic resonance can contribute slightly to the high field permeability because the breadth of the ferromagnetic resonance for iron is large.

Eddy currents will also contribute to high field loss because even though the permeability from other sources approaches unity, currents are induced in the conductive particles. In this case, the real part of the permeability should become negative (i.e., the frequency shift as plotted in Figs. 18-34 should become negative). Clearly, that does not happen.

4.2 Coating Geometry and Orientation (a Cautionary Note)

One effect that will prove to be important is the coating geometry and its orientation with respect to the magnetic field. This occurs because of the effects of demagnetization as described earlier. As was shown, the sample permeability is a function of the applied magnetic field. However, more correctly, the magnetization of the sample is a function of the applied magnetic field within the sample. For example, Fig. 35 shows the magnetization of a sample of about 40% by volume CIP in a slab about $0.5 \times 0.5 \times 0.06$ cm. Curve (a) shows the magnetization when the applied magnetic field is parallel to the 0.5×0.5 cm plane. The sample reaches saturation at about 6 kOe. However, when the applied magnetic field is perpendicular to that plane, the sample does not reach saturation even at 10 kOe.

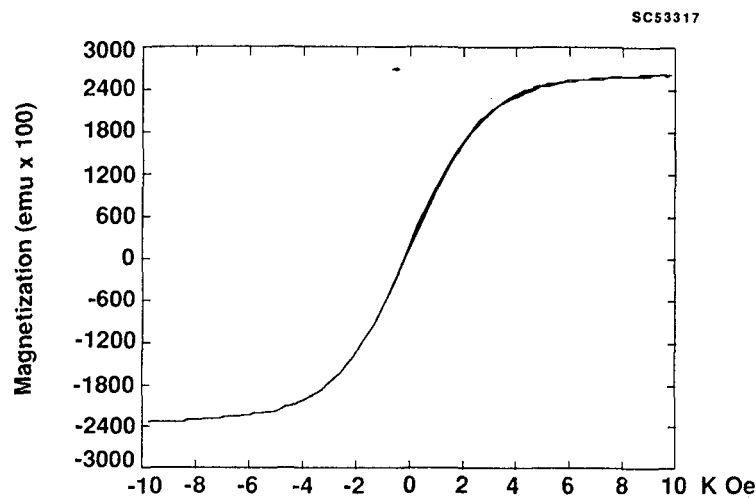
The internal field, H_I , is given by the applied field, H , less the demagnetization field which is equal to the sample magnetization multiplied by the demagnetization factor,

$$H_I = H - DM \quad (19)$$

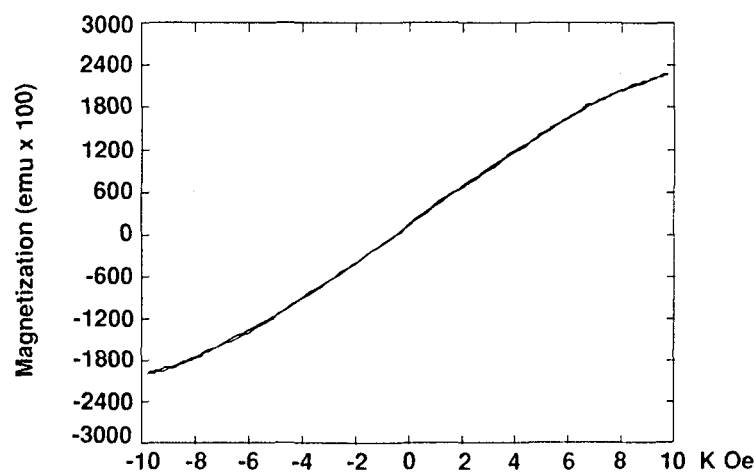
Strictly speaking, for any nonellipsoidal shape the demagnetization field is not constant throughout the body so that in practice average values or those of similar ellipsoidal bodies are used. Thus, accurate demagnetization factors cannot be calculated for either composite media such as carbonyl iron in polymeric matrices⁸ or for nonellipsoidal



SC73001.FR



a.



b.

Fig. 35 Magnetization of approximately 40% by volume of carbonyl iron in a polymeric matrix of about $0.6 \times 1.2 \times 0.055$ cm: (a) magnetization vs applied field for the sample oriented parallel to the applied field; and (b) magnetization vs applied field for the sample oriented perpendicular to the applied field.



bodies.⁹ Based on this research the demagnetization factor is expected to be a function of the permeability of the material, the geometry, and the degree of saturation.

Therefore, the internal fields of dilute mixtures of carbonyl iron particles can be calculated from the properties of the individual particles, whereas those of more concentrated mixtures cannot.

From a qualitative point of view, one can consider the charts in Fig. 35. An oblate ellipsoid with relative dimensions of $a:b:c = 1:0.5:0.046$ should exhibit demagnetization factors of 0.03, 0.07, and 0.90 when the magnetic field is aligned, respectively, along the a, b, and c directions. Using this coordinate system Fig. 35(a) represents the field aligned parallel to the "b" direction of the sample, and Fig. 35(b) shows the magnetic field is aligned parallel to the "c" direction. Assuming 40% by volume of iron, so that $4\pi M_S$ for the sample is 8344 Gauss, at saturation the demagnetizing fields are about 600 and 7400 Oe respectively for Figs. 35(a) and 35(b). This illustrates the strong effect of orientation with respect to the magnetic field.

Clearly, when the coating is perpendicular to the applied field, larger "DC" fields could be applied to the sample before saturation is reached. Thus, in a practical system, if the field direction could be arranged so that the field is normal or near normal to the surface, a wider range of performance will be obtained.

4.3 Conclusions

The results of the measurements show that carbonyl iron powders can be used as microwave absorbing materials at magnetic fields greater than 3 kOe, and depending on orientation of the coating with respect to magnetic field, fields greater than 6 kOe may be reasonable. The performance at a given applied magnetic field will depend to some extent on the CIP material, but largely on the orientation of the coating with respect to the applied field.

The best materials in terms of performance with respect to large magnetic fields are SF, which appeared to be the best behaved, followed closely by HFQ, E, and EW. TH powder, made by GAF, is slightly finer than type E, would also be expected to



fall into this group. Other powders, such as KX which are larger than the others, or those chemically treated, such as GS-6 and W, did not exhibit such good performance.

The concentration of CIP is less important, but can be important if high concentrations are used because the demagnetization fields will be more affected by the overall sample geometry. For dilute systems, the particles behave as independent, noninteracting spheres.

Values of μ' and μ'' are both magnetic field and microwave frequency dependent. Thus constant performance will not be obtained at all applied magnetic fields. Rather, calibrations will probably need to be run for a particular geometry.



5.0 RECOMMENDATIONS

5.1 Material and CIP Concentration

1. Although there are not large differences among the CIP powders tested, certain aspects make some materials preferable over others. As can be seen from transmission line measurements, the field dependence of μ' and μ'' differ at different frequencies. Thus, it is best to determine the range of frequencies over which optimal performance is required, and then design and test appropriate absorbers.
2. Concentration alone is not a significant factor other than that it affects the thickness and maximum attenuation. As a guide, the largest concentration that could be used will give the best results, but only if fields below about 3 kOe are used or if the coating could be oriented perpendicular to the applied field. Thus, once good absorbing materials are selected, they should be tested on representative geometric shapes placed in a magnetic field.
3. If fields are to be greater than about 3 kOe, and the direction of the coating cannot be controlled, more dilute but thicker layers would be advantageous.

5.2 Measurements

Before a large investment is made in time and materials for a prototype system, if such is planned, a number of measurements should be made. The test matrix should include:

- Coatings of different CIP types, concentrations and thicknesses.
- Different geometric solids (ie. sphere, cylinder ogive, corner).
- Orientation of the solid with respect to the applied field.
- Different applied fields up to the desired value.
- Measurement over high priority frequency ranges.



The most important factor is not whether the magnetic field is homogeneous, but is the orientation of the coating with respect to the field.

Several approaches can be used to accomplish these measurements with existing equipment. The pole pieces of the electromagnet used in this study can be removed to provide a cylindrical magnetic field region of about 15" in diameter by about 8" thickness. In this configuration, the magnetic field is parallel to the axis of the cylinder. The maximum field in this configuration is greater than 7 kOe. The microwave transmission direction would be parallel to the 15" ends of the cylinder. For narrow bands (± 10 -15%) of frequencies above 8.5 GHz, the components of the electromagnet can be covered with standard flat carbon impregnated foam, and focussed horns can be used to maximize the microwave energy on the test sample. A recent addition to this facility is an X-band horn-lens that will focus more than 80% of the microwave energy in an 8" diameter beam. Other focussed or collimated beam horn lens antennae at frequencies above 14 GHz are available.

For lower frequencies or to cover a broad frequency range where it is less convenient to focus energy into a narrow region, broad band horns can be used. In such cases thin smooth aluminum plates could be mounted on the surface of the electromagnet to minimize specular reflection near the sample. The microwave reflection from the sample is then gated over narrow time limits to reduce clutter. This is easily accomplished with the available Hewlett-Packard Model 8510-B Automatic Vector Network Analyzer.

Such measurements can be used to design the best absorber. For a thorough evaluation, some performance criteria would need to be set. Such criteria should include whether uniform or maximum performance is most desirable, the key frequency regions in which the material should perform, whether thickness is of major concern, and a prioritized ranking of frequency. It would also be important to establish one or several representative standard geometries for the test system.



6.0 REFERENCES

1. J. Verweel, "Ferrites at Radio Frequencies," in J. Smit, Ed., **Magnetic Properties of Materials**, Chapter 3, McGraw-Hill, NY 1971.
2. J. Verweel, in **Magnetic Properties of Materials**, J. Smit, Ed., McGraw Hill, NY, 1971, Chapter 3.
3. S. Chikazumi and S.H. Charap, **Physics of Magnetism**, R.E. Kreiger, Malibar, FL 1978, Jophn Wiley and Sons, 1964.
4. C.J. Larson, "A Frequency Domain Metrology System for Measuring Permittivity and Permeability," in 1980 Radar Camouflage Sympos., Orlando FL, 1980, pp 131-141.
5. "Measuring Dielectric Constant with the HP 8510 Network Analyzer: The Measurement of Both Permittivity and Permeability of Solid Materials," Product Note 8510-3, Hewlett Packard, Palo Alto, CA, Aug. 1965.
6. W.B. Weir, Proc. IEEE, **62**, 33-36 (1974).
7. B. Lax and K.J. Button, **Microwave Ferrites and Ferrimagnetics**, McGraw Hill, NY, 1962.
8. I.B. Goldberg and R. Goldfarb, unpublished work.
9. D.X. Chen, J.A. Brug, and R.B. Goldfarb, "Demagnetization Factors of Cylinders," IEEE Trans. Magn., in press.



APPENDIX I BIBLIOGRAPHY ON MICROWAVE MAGNETICS

General Magnetism

R.M. Bozorth, **Ferromagnetism**, Van Nostrand, New York, 1951.

Comprehensive summary of magnetic properties of materials to 1950. Not much information on thin films or microwave properties. Excellent discussion of the relationship of the structure of materials to their magnetic properties. Very readable text.

S. Chikazumi and S. H. Charap, **Physics of Magnetism**, R. E. Krieger, Malabar, FL, 1978; John Wiley and Sons, New York, 1964.

Excellent description of magnetic phenomena and a good section on ferromagnetic resonance. The magnetic phenomena are explained clearly starting at introductory level and progressing through mathematical treatments.

B.D. Cullity, **Introduction to Magnetic Materials**, Addison Wesley, Reading, MA, 1972.

This is probably the best textbook for a general understanding of magnetism without "excessive" mathematics. The book has good discussions of measurement techniques, and uses magnetic properties of materials to illustrate different effects. It was written for "materials scientists." Does not have much explanation of electromagnetic properties.

J.P. Jakubovics, **Magnetism and Magnetic Materials**, Institute of Metals, London, 1987.

Descriptive or semi-qualitative discussion of magnetic phenomena, the book is somewhat more informative than Kaganov's book described below. The first part provides descriptions of magnetic phenomena; the second part presents materials for general applications. The book contains few details on specific properties, materials, or applications. There is no information on microwave materials. Most of the book is easy to read anywhere. Although it is a good introduction, its price tag (\$32.00 for 138 pg. paperback) takes this out of range of most personal collections.

M.I. Kaganov and V. M. Tsukernik, **The Nature of Magnetism**, Mir Publishers, Moscow, USSR, 1895.

Descriptive or semi-qualitative discussion of magnetic phenomena. Little detail of materials' properties or electromagnetics. Equations are explained rather than derived. The facts that the book is paperback size and costs about \$5 makes it worthwhile and easy to read on a bus, train airplane or carpool. There are some rough spots because of the translation.

A. H. Morrish, **The Physical Principles of Magnetism**, R. E. Krieger, Malabar, FL, 1983; John Wiley and Sons, New York, 1965.

This is the most theoretical of the books cited. The text is clearly written from a general physics viewpoint rather than materials science or engineering, but is not rigorous. The discussions of magnetic phenomena include examples of materials. Fairly comprehensive treatment of electromagnetic effects.



R. F. Soohoo, **Magnetic Thin Films**, Harper & Row, New York, 1965.

This book provides an excellent summary of the magnetics of thin films. It is a very comprehensive analysis of single layer magnetic films, and includes magnetostatics, domain effects, and ferromagnetic resonance. It is somewhat outdated. The text does not cover multilayer film structures.

Microwave Magnetics:

A. J. Baden-Fuller, **Ferrites at Microwave Frequencies**, Peter Peregrinus Ltd. (on Behalf of IEE, London, UK, 1987.

This book provides a summary of theory of magnetics relevant to high frequencies and describes various measurements techniques and devices that incorporate ferrites. It does not provide detail, references to specific materials or any discussion relevant to the workshop subject. One good feature of the book is that because it is new, it covers subjects of current interest and activity, and it is available.

P. J. B. Clarricoats, **Microwave Ferrites**, John Wiley and Sons, New York, 1961.

This was found in an old book store at the same time as Waldron, below, and I haven't had a chance to read it. A cursory glance shows it has very relevant topics and a fairly comprehensive theoretical discussion relevant to this workshop, including domain and ferromagnetic resonance losses. The book deals with insulating magnetic materials, therefore there are no eddy current effects.

B. Lax and K. J. Button, **Microwave Ferrites and Ferrimagnetics**, McGraw-Hill, New York, 1962.

This book is the classic in the field. If you find a copy, try to get it. It contains almost every aspect relevant to microwave magnetics except eddy current effects. The text is extremely well written and referenced, and the theoretical aspects are carefully derived, but more important, clearly explained. My bias is obvious!!!!

R. F. Soohoo, **Microwave Magnetics**, Harper & Row, New York, 1984; may be available as a reprint from R. E. Krieger, Malibar, FL.

A good survey of microwave magnetics and reasonably readable. It does not provide great detail, but has broad coverage of the primary applications of magnetic materials in microwave devices. Some measurement techniques are described. The book is most current of all mentioned.

W. H. von Aulock and C. E. Fay, **Linear Ferrite Devices for Microwave Applications**, Academic Press, New York, 1968.

A good device book, it does not have as much detail as Waldron or Clarricoats.

R. A. Waldron, **Ferrites, An Introduction for Microwave Engineers**, Van Nostrand, Princeton, N. J., 1961.

This was found in an old book store at the same time as Clarricoats, above, and I haven't had a chance to read it in detail. A cursory glance shows it has very relevant topics and a fairly comprehensive theoretical discussion relevant to this workshop. Topics that are treated in detail include cavity perturbation theory [an area in which Waldron is an



authority] , ferromagnetic resonance, and devices. The book deals with insulating magnetic materials, therefore there are no eddy current effects.

Ferrites and magnetic materials:

F.N. Bradley, **Materials for Magnetic Functions**, Hayden, New York, 1971.

A good introductory book to the chemistry and structure of magnetic materials and device applications. It does not have much specific detail or theory. It is extremely easy to read, and relatively little physics or mathematics background is needed to understand to text. Lots of figures and diagrams.

C.-W. Chen, **Magnetism and Metallurgy of Soft Magnetic Materials**, Dover, Mineola, NY 1986; North Holland, Amsterdam, 1977.

Good discussion of the relationship of the structure and chemistry of materials to their magnetic properties. Materials described are relevant to this topic. Reasonably easy to read.

J. Smit, ed. **Magnetic Properties of Materials**, McGraw-Hill, New York, 1971.

Although the book presents an overview of magnetics, it is centered around ferrites. There is a good section on ferromagnetic resonance. The book is mostly qualitative and very well written.

J. Smit and H.P.J. Wijn, **Ferrites**, John Wiley and Sons, New York, 1959.

This book is another classic in the field. It provides an excellent basic or introductory section on magnetism and magnetic effects, including domain wall motion, ferromagnetic resonance, and types of magnetic materials. It was written before ferromagnetic resonance became a significant topic. The discussion of ferrites in terms of classification of materials, characteristics, behavior and preparation is excellent. It is well written.

R.F. Soohoo, **Theory and Application of Ferrites**, Prentice Hall, Englewood Cliffs, N.J., 1960.

This book provides a good balance between theory and application of ferrites. The first part provides basic theory of magnetic materials with an emphasis on ferrites. It is one of the few places where dielectric properties of magnetic materials are discussed. The second part presents a summary of applications of ferrites. The book is generally well written; however, some equations are given without interpretation or derivation.

W.H. von Aulock, ed., **Handbook of Microwave Ferrite Materials**, Academic Press, New York, 1965.

This book provides a good simple description of the behavior of ferrites and different classes of materials. It then provides data on a wide range of ferrite materials organized by class of ferrite. It is out of date, but useful.



Electromagnetic Waves and Magnetism:

R. Becker, **Electromagnetic Fields and Interactions**, Dover, New York, 1982; Blaisdell, New York, 1964.

Good reference, but more detail than is needed here.

S. Ramo, J.R. Whinnery, and T. van Duzer, **Fields and Waves in Communication Electronics**, 2nd Ed., John Wiley & Sons, New York, 1984.

Of all the books in this category, this is the one that is most generally recommended. It contains a strong discussion of most aspects of electromagnetic waves and interaction with materials. One advantage is that it is self-contained; i.e., all of the mathematics needed are described in the book.

J. A. Stratton, **Electromagnetic Theory**, McGraw-Hill, New York, 1941.

This book is outdated but remains the classic in the field. It is primarily theoretical and provides excellent background for calculating the interaction of a wave with any material based on the fundamental properties of the material. It is not particularly easy to read, but it is very comprehensive.



3 1176 01413 7013



Rockwell International
Science Center

... where science gets down to business